



Contents lists available at SciVerse ScienceDirect

Tectonophysics

journal homepage: www.elsevier.com/locate/tecto

Brittle tectonic evolution along the western margin of South Africa: More than 500 Myr of continued reactivation

G. Viola ^{a,b,*}, A. Kounov ^c, M.A.G. Andreoli ^{d,e}, J. Mattila ^f

^a Geological Survey of Norway, NGU, Leiv Eirikssons vei 39, 7491, Trondheim, Norway

^b Department of Geology and Mineral Resources Engineering, Norwegian University of Science and Technology, 7491 Trondheim, Norway

^c Institute of Geology and Paleontology, Basel University, 4056 Basel, Switzerland

^d South African Nuclear Energy Corporation, Necsa, PO Box 582 Pretoria 0001, South Africa

^e School of Geosciences, University of the Witwatersrand, Private Bag 3, 2050 Wits, South Africa

^f Geological Survey of Finland, GTK, P.O. Box 96, FI-02151, Espoo, Finland

ARTICLE INFO

Article history:

Received 23 June 2011

Received in revised form 6 October 2011

Accepted 8 October 2011

Available online xxxx

Keywords:

Brittle deformation

Paleostress tensor inversion

Passive margin evolution

South Atlantic

ABSTRACT

The brittle structural history of western South Africa has been investigated by remote sensing and field studies to build a conceptual scheme for its >500 Ma long evolution. Paleostress tensors were computed from a significant fault-slip dataset and a relative geochronological succession of brittle deformation events was established. This was aided by separating in time faulting events through the usage of Cretaceous weathering horizons, silicified fluvial deposits, paleosols and 77–54 Ma olivine melilitite plugs as time markers. The oldest features recognized formed during four compressional episodes assigned to the Neoproterozoic Pan African evolution. This history is expressed by sub-vertical conjugate fracture sets and fits well the inferences derived from remote sensing. The greatest compressive direction rotated from NW–SE to NNE–SSW and finally to almost E–W. A subsequent ENE–WSW-oriented extensional episode is associated with the local effects of the opening of the Atlantic Ocean and was followed by a second, ca. E–W extensional episode, linked to the well-acknowledged Mid-Cretaceous (115–90 Ma) event of margin uplift. A late Santonian (85–83 Ma) NW–SE compressive paleostress deformed the Late Cretaceous sequences and was in turn followed firstly by a renewed episode of NE–SW extension and later by ca. NNE–SSW Late Maastrichtian (69–65 Ma) shortening. The latter is broadly coeval with the emplacement of the Gamoeep magmatic suite. A phase of WNW–ESE Cenozoic extension is assigned to the extensional phase recorded in the Okavango delta, interpreted as reflecting propagation of the East African Rift System into southern Africa. No stress tensor was computed for the present day “Wegener anomaly” stress field, oriented NW–SE. However, *in situ* stress measurements were used to perform slip tendency analysis, which indicates that, under the currently existing stress conditions, WNW–ESE- and NNW–SSE-striking faults are critically stressed and are the most likely reactivated, in agreement with the present seismicity.

© 2011 Elsevier B.V. All rights reserved.

1. Introduction

Old cratonic crystalline basements usually present compelling evidence of complex brittle deformation histories. Unfortunately, their typically long geological evolution and the repeated structural reactivation of inherited structures can obliterate fully or partially much of the information that is necessary to unravel these histories.

Munier and Talbot (1993), for example, showed that the Precambrian basement of southeast Sweden is fully saturated of fractures and they derived a statement of general validity wherein the ratio between fragmentation (i.e. generation of new fractures) to jostling (i.e. reactivation of old fractures) in old terranes decreases with

time in response to the partial (if not total) accommodation of every new deformational episode by preexisting structures. Despite the structural complexities resulting from this, Viola et al. (2009) and Sainot et al. (2011) showed that it is actually possible to unravel the extremely long and complex brittle history of the Fennoscandian Shield by an integrated structural approach consisting of a detailed geometric and kinematic study of striated fault planes and brittle fault rocks analysis. They proposed a paleostress vs. time chart for two different areas in southwest Sweden that covers more than 1.5 and 1.7 Ga of brittle structural history, respectively.

Inspired by a similar approach, and aiming at the same time at a better understanding of strain localization and structural reactivation in old metamorphic terranes, we present here the results of a study that focuses on the brittle deformational history of part of Namaqualand, western South Africa (Fig. 1). At Vaalputs, in the heart of Namaqualand (Figs. 1 and 2), the South African Nuclear Energy Corporation (Necsa)

* Corresponding author at: Geological Survey of Norway, NGU, 7491 Trondheim, Norway. Tel.: +47 73 90 42 36; fax: +47 73 92 16 20.

E-mail address: giulio.viola@ngu.no (G. Viola).

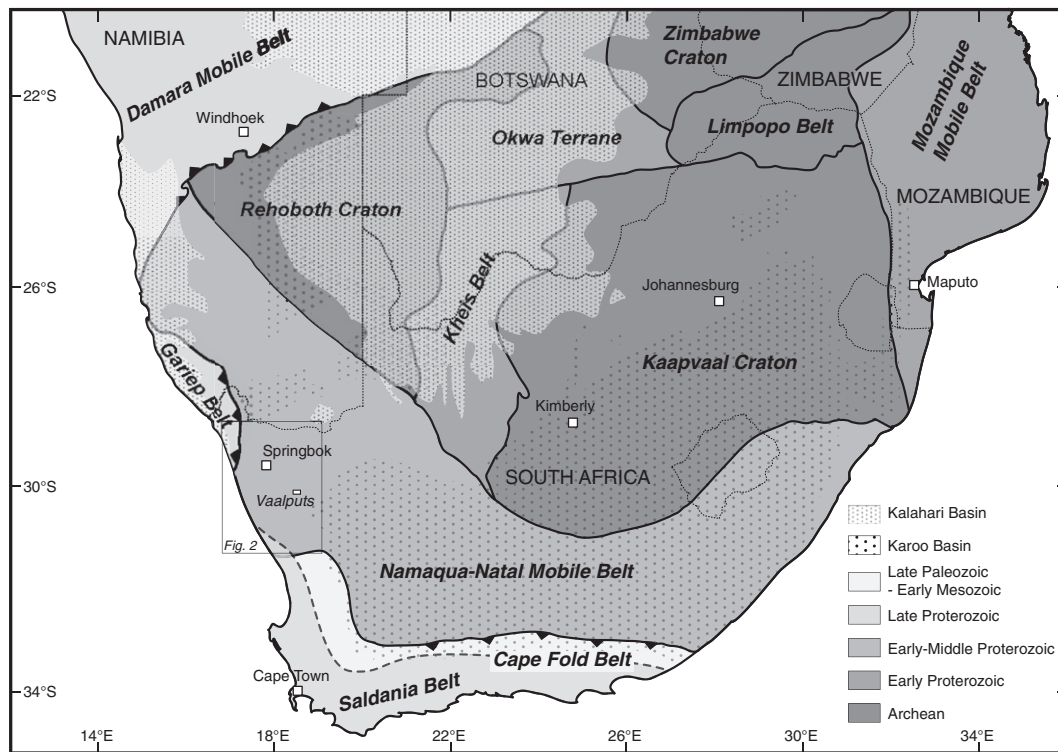


Fig. 1. Main constitutive tectonic elements of southern Africa. The study area is framed by a rectangle and zoomed into in Fig. 2.

operates a site licensed for the disposal of low- and intermediate-level radioactive waste in ca. 7 m deep trenches (e.g. Brandt et al., 2005). Although the geology of the region has been the subject of numerous in depth studies (see Cornell et al., 2006 for a recent review), the structural framework of the area and its brittle component in particular remain poorly explored and understood. In this study we propose a new conceptual structural scheme for Namaqualand's long brittle structural evolution, based primarily on the analysis of selected brittle structures. Key components of this analysis included both remote sensing and fieldwork to gather sufficient fault-slip data to generate a statistically robust reconstruction of the paleostress evolution of the region. Indirect time constraints were obtained through the analysis and comparison of the deformation episodes that affected lithologies of known age and by the unraveling of crosscutting relationships among different sets of structures. This approach also made it possible to add constraints to the brittle evolution of the region during the geologically fundamental process of the opening and the evolution of the South Atlantic Ocean. Finally, we have also computed fault-slip tendency analysis to better understand the behavior and the role of inherited brittle structures within the present-day stress field, and thus the control they may exert on the current seismicity of western southern Africa.

2. Regional geologic setting

2.1. Geological background

The western coast of South Africa is characterized by the occurrence of diverse lithologies, from Proterozoic metamorphic rocks to Neoproterozoic and Mesozoic sedimentary and igneous sequences (Fig. 1). The Mesoproterozoic Namaqualand Metamorphic Province (NMP), part of the Namaqua-Natal Mobile Belt (Fig. 1), comprises intensely deformed supracrustal sequences intruded by numerous pre-, syn- and post-tectonic granitoids (Fig. 2; e.g. Johnson et al., 2006). Exhumation of the NMP rocks during the Early Neoproterozoic (between 1000 and 800 Ma) was followed by deposition of the Gariep Supergroup in a pull-apart basin (Gresse, 1995). The sediments of the Neoproterozoic-

Cambrian Vanrhynsdorp Group unconformably overlie the Gariep Supergroup (Johnson et al., 2006; Fig. 2). The Vanrhynsdorp and Gariep Group rocks were deformed and metamorphosed during the Pan-African orogeny between 650 and ca. 500 Ma at relatively low temperatures. Based on ^{40}Ar - ^{39}Ar cooling ages (Frimmel and Frank, 1998; Gresse et al., 1988; Reid et al., 1991), it can be argued that most of the region studied here entered the brittle realm by ca. 500 Ma. However, lateral/local differences in the cooling pattern might have occurred depending on the distance from the Pan African orogenic front and the presence of discrete, fluid-permeable shear zones (e.g. Frimmel and Frank, 1998).

The Meso- and Neoproterozoic rocks are unconformably overlain by the Ordovician–Devonian thick siliciclastic sequences of the Cape Supergroup (Fig. 2; Johnson et al., 2006). From the late Carboniferous to the Early Jurassic, the Karoo Supergroup, which consists of several kilometers of clastic sediments, was deposited in the Karoo Basin (Fig. 1). This is considered as a foreland basin, possibly formed in response to orogenic loading of the Cape Fold Belt to the south (Johnson et al., 2006). The Cape Fold Belt, a component of the Gondwanides chain, formed during mostly Triassic crustal shortening related to the subduction and accretion of the paleo-Pacific plate beneath Gondwana (de Wit and Ransome, 1992). The break-up of Gondwana (ca. 170–150 Ma; Hawkesworth et al., 1999) started with the separation of west Gondwana (Africa and South America) from east Gondwana (Australia, Antarctica, India and New Zealand), following the extrusion of the voluminous and extensive continental flood basalts of the Drakensberg Group (184–174 Ma; Jourdan et al., 2007) and, close to the study area, the emplacement of numerous dolerite sills (Karoo magmatic event). The subsequent break-up of west Gondwana between 144 and 125 Ma started with rifting accompanied, along the margin, by the intrusion of syenite and granite plutons, as well as dolerite dykes (e.g. Eales et al., 1984; Reid and Rex, 1994; Trumbull et al., 2007). In the southern Atlantic, the rift–drift transition was marked by the northward propagation of the spreading center over a period of around 40 Myr, with sea-floor spreading beginning at about 134 Ma (Eagles, 2007; Rabinovich and LaBrecque, 1979).

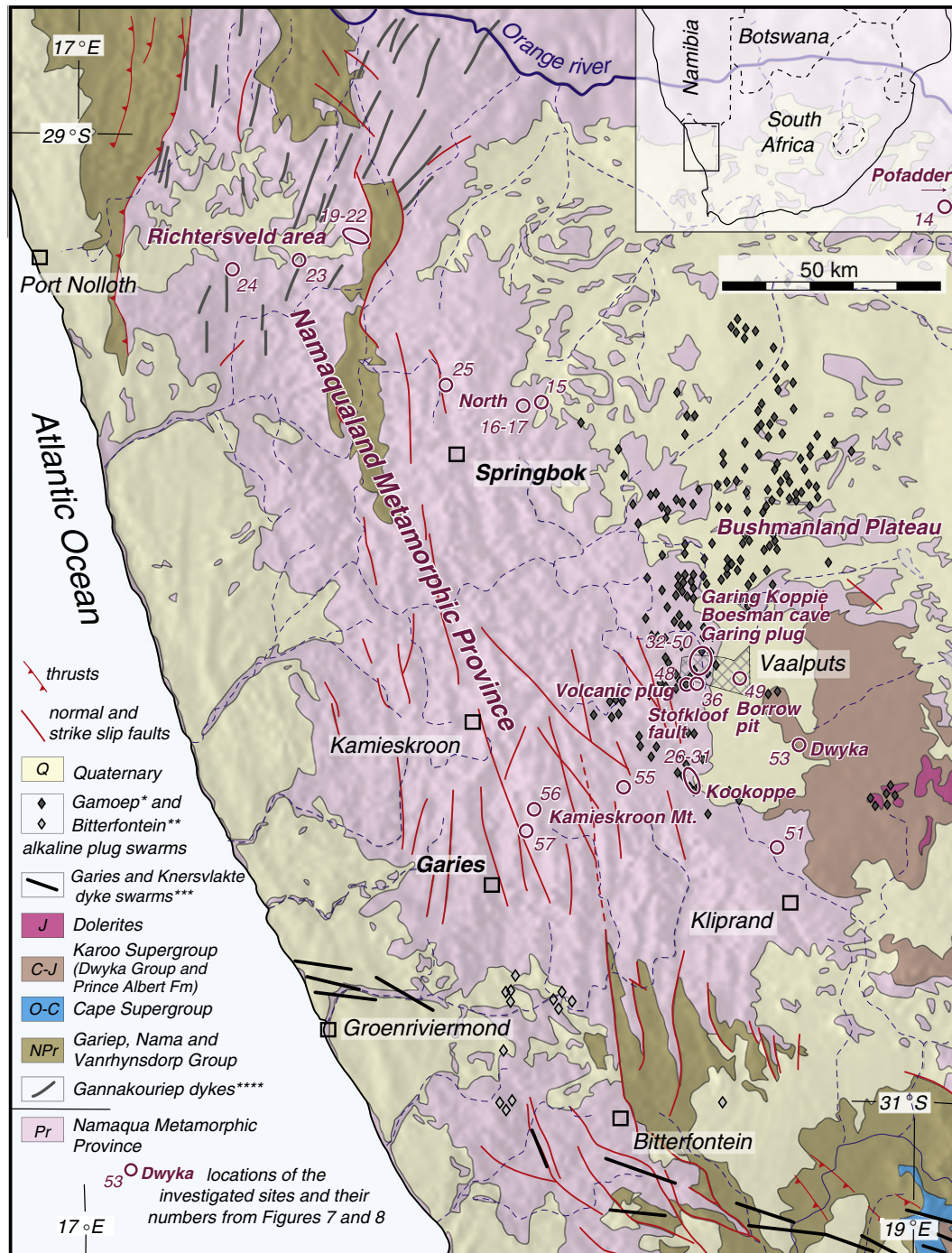


Fig. 2. Geological map of the Namaqualand area draped on the local digital elevation model. The outline of the farm Vaalputs is shown. Observation localities are indicated by a numerical code or a label that refers to Fig. 9. Asterisks refer to the available ages of volcanic alkaline plugs and doleritic dykes. *: plug age between ~77 and ~54 Ma (Phillips et al., 2000); **: plug age between 56 and 38 Ma (Phillips et al., 2000); ***: dyke age of 134 ± 3 Ma (Reid and Rex, 1994); ****: dyke age of 717 ± 11 Ma (Reid et al., 1991).

Concomitant with the early drift phase, numerous mafic alkaline intrusions, including kimberlites and related rocks, intruded across southern Africa. Two distinct intrusion peaks have been reported at 145–115 and 95–80 Ma, corresponding to kimberlite Group II and I, respectively (e.g. Basson and Viola, 2004; Smith et al., 1985). Two further clusters of kimberlitic plugs were later emplaced in our study area, the older (~77–54 Ma) near Vaalputs (Gamoep cluster) and the younger (56–38 Ma) ca. 50 km to the SSW, near Garies (Bitterfontein cluster; Fig. 2; Phillips et al., 2000).

In the study area only small patches of Cretaceous sediments are observed (Dasdap Formation, see below), whereas a wide range of

Cenozoic sedimentary deposits cover the low coastal plain (Fig. 2). Raised marine terraces, often rich in placer diamonds and occurring at various elevations along the coast, have been linked to Miocene, Pliocene and Quaternary transgressions (Pether et al., 2000).

2.2. Geomorphic evolution

In the Namaqualand area, the coastal plain is separated by a broad and deeply incised highland region (the Namaqualand Escarpment) from the predominantly featureless, rolling plain that extends inland at an altitude of ~1000 m a.s.l. (Fig. 2). The latter was named the

Bushmanland Plateau by Mabbutt (1955), and later attributed to the Late Cretaceous–Early Cenozoic “African” planation surface (e.g. King and King, 1959; McCarthy et al., 1985; Partridge and Maud, 1987). Semiarid, and home to a sparse population, the Bushmanland Plateau conforms to the requirements for the safe disposal at Vaalputs of low- and intermediate-level radioactive waste (e.g. Brynard, 1988; Brynard et al., 1996; Levin, 1988). The plateau represents the westernmost sector of the elevated margin of African subcontinent. It currently attracts considerable scientific interest because it is part of the broad region of elevated topography that overlies the low-velocity zone mapped at the lower mantle-core boundary, called the African Superswell (Lithgow-Bertelloni and Silver, 1998; Nyblade and Robinson, 1994).

The Namaqualand Escarpment is dominated by a rugged and mountainous landscape of granitic rocks rising in places to more than 700 m above the plateau. In this area, sandy pediments with more gentle slopes merge into valley floors that are deeply incised and largely controlled by geological structure, following faults and other lineaments (Fig. 2). The origin of this deeply-incised geomorphic feature is contentious, and may represent the relic of the Late Jurassic elevated shoulders that framed the proto-Atlantic rift (Partridge and Maud, 1987). Alternatively, the highlands have been interpreted as remnants of a post-rift, easterly-migrating bulge arising from the isostatic adjustment of the continental margin to the retreat of the escarpment (Brandt et al., 2005; Gilchrist et al., 1994; Kooi and Beaumont, 1994). Recently, low-temperature thermochronological studies have indicated a component of tectonically induced late Cretaceous uplift in the area of the Namaqualand Escarpment (Brown, 1992; Kounov et al., 2009).

3. Stratigraphy of the study area

Below we describe in more detail the tectonostratigraphic units that crop out in the study area and which were pivotal to the establishment of the time sequence of brittle deformational events proposed in our model. The section of Fig. 3 illustrates a schematic view of the most significant stratigraphic relationships observed.

3.1. Namaqua Metamorphic Province

The investigated Namaqua Metamorphic Province is part of a granulite, granite and charnockite belt exceptionally enriched in U and Th (Andreoli et al., 2006). These rocks experienced high temperature, intermediate pressure granulite-facies metamorphism (T: 800–860 °C and P: ~5–6 kbar) during the Grenvillian orogeny ca. 1030 Ma ago (Waters, 1989). To the west, along the Atlantic coast, the Namaqua gneisses bear lower grade (staurolite zone) mineral assemblages indicating a tectonic-metamorphic overprint during the ~550–500 Ma Pan African orogeny (e.g. Frimmel, 2000). The escarpment area to the west of the Bushmanland Plateau is dissected by a swarm of generally NNW-striking, brittle–ductile to brittle faults clearly discernible in

Landsat satellite imagery as deeply incised valleys, which are one of the targets of our study (see below).

3.2. Karoo Supergroup sediments

Late Carboniferous to the Early Jurassic Karoo sediments cover presently almost one third of South Africa (Fig. 1) and in the study area they are represented mainly by Late Carboniferous–Early Permian tillites of the Dwyka Group (Fig. 2). These are only seldom exposed on the Bushmanland Plateau around the Vaalputs site, but become increasingly exposed eastward (Fig. 2). An important feature of all Karoo rocks exposed in the region is their highly indurated nature, which in turn allows the preservation of joints and fractures. Sets of NNW-trending reactivated and often conjugate faults dissect both the Permian Dwyka Group and the overlying Triassic Prince Albert Formation over a broad area NE of Vaalputs. No Jurassic dolerites are reported from the Vaalputs area.

3.3. Cretaceous–Palaeocene lithological sequences

Scattered outcrops of lithological sequences from this time interval are exposed only along a narrow belt at the transition between the Bushmanland Plateau and the Namaqua escarpment. Their importance cannot be overlooked because, in addition to testifying to events for which the record has been largely lost over most of South Africa, these rocks are also extremely useful in our study in that they provide key time markers. They are typically found on or close to silicified mesas, and include the alluvial fan sequence of the Dasdap Formation (Figs. 3 and 4a; Brandt et al., 2003), scattered outcrops of tropical regoliths, and a swarm of ultramafic alkaline pipes and their craters often recognizable by the sedimentary or breccia in-fills. The Dasdap Formation is a relic of a high energy, erosional-depositional cycle laid on the retreating, rifted continental margin under the tropical, humid conditions of the Late Cretaceous (Brandt et al., 2003; Kounov et al., 2009; Partridge and Maud, 1989, and references therein). Likewise, the regoliths comprise a variety of different facies such as hillside scree deposits, nodular ferricretes (palaeosols), and silcrete-kaolinite profiles typical of tropical, humid conditions (Fig. 4; Brandt et al., 2005; McCarthy et al., 1985; Partridge and Maud, 1989, 2000).

By the end of the Cretaceous to the beginning of the Paleogene, the region was intruded by a great number of kimberlite/and olivine-melilitite basalt pipes of the so-called Gamoe cluster (Fig. 2; Cornelissen and Verwoerd, 1975). Scarce dating of these volcanic rocks gives ages between 77 and 54 Ma (cf. Moore and Verwoerd, 1985; Phillips et al., 2000). Haughton (1931) proposed an age between the Late Cretaceous and the Early Tertiary based on fossil frogs found in the infill of one of the pipes. Later studies focussing on the palynology of these infill sediments, proposed the Early Paleocene as the age of the infill (64–54 Ma). We have analyzed some pipe occurrences of Late Cretaceous age in the Vaalputs area that can be assigned with confidence to the Gamoe suite. The volcanic pipes are found as actual

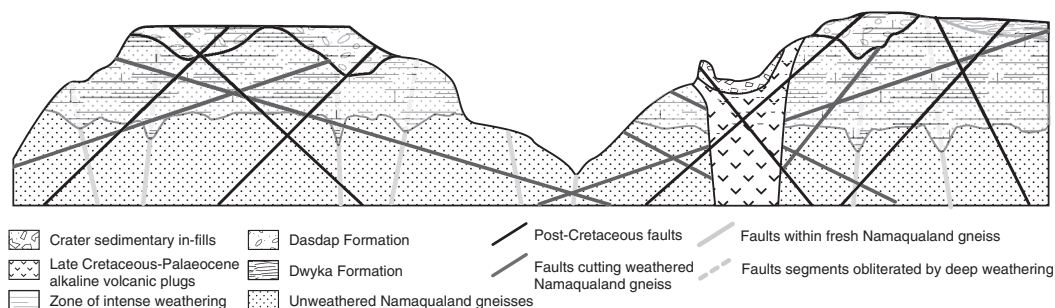


Fig. 3. Representative section showing the stratigraphic relationships observed within the study area. Faults belonging to different generations are indicated. Section not drawn to scale.

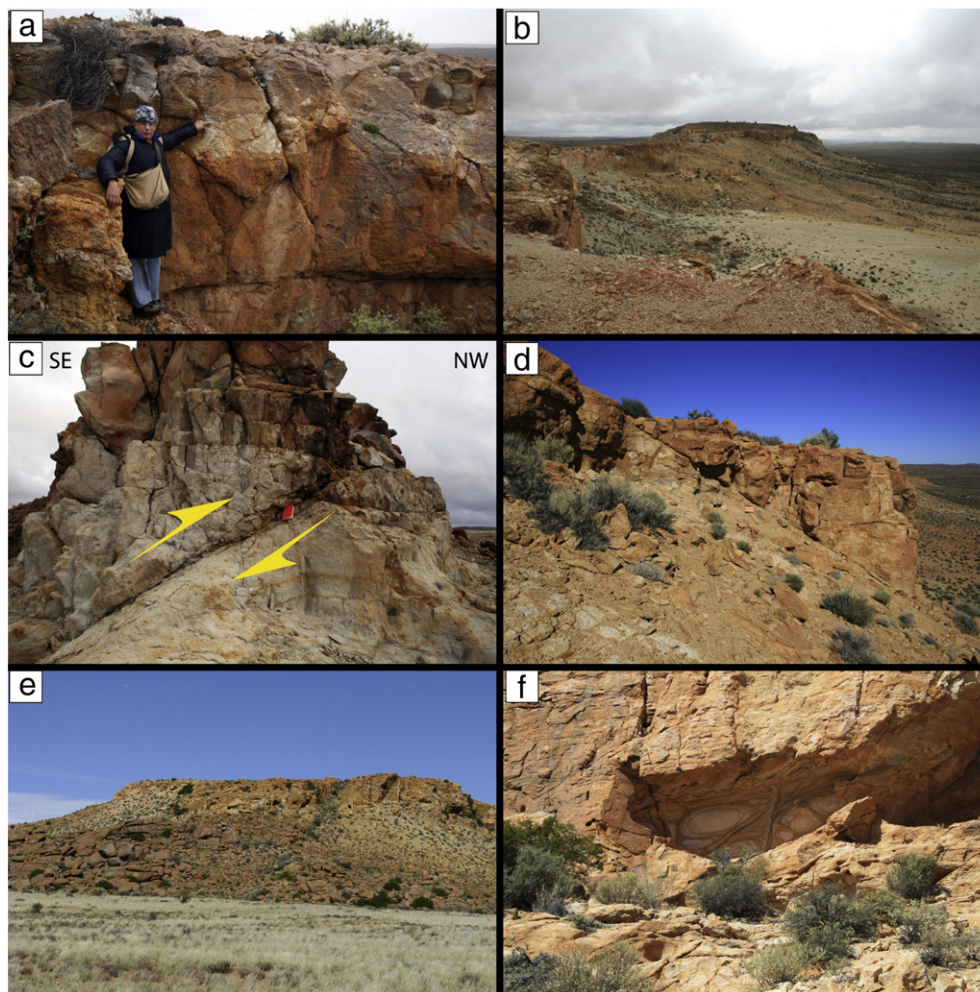


Fig. 4. Examples of Cretaceous–Paleocene rocks and morphotectonic features from eastern Namaqualand. a): Basal unconformity separating the highly weathered Namaqua basement from the basal conglomerate-coarse immature sandstones of the Late Cretaceous Dasdap Formation (Brandt et al., 2003; coordinates: 30° 20.360', 18° 27.062'). b): View to the north of the mesa of Kookoppe (Fig. 2 for its location), formed by the weathered metamorphic basement and sandstones of the Dasdap formation. c) and d): Evidence of tectonism affecting Late Cretaceous rocks and morphological features: c): Discrete, ca. top-to-the-NW thrust plane (42/138, dip and dip direction) that deforms Dasdap formation sandstones (30° 20.147', 18° 27.002'). d): Highly weathered metamorphic basement dissected by discrete fractures and a sharp thrust plane. e): Hillock of metamorphic basement showing the depth extent of the yellow-looking weathering front affecting its top. f): Example of fracture-controlled weathering (conceptually shown also in Fig. 3). Corestones with onion-type exfoliation patterns are formed within rock volumes bound by discrete fracture planes that act as conduits for the weathering fluids.

basaltic plugs, as breccia pipes and as often oval to elongated patches of arenaceous pipe-fill sediments surrounded by basement (Cornelissen and Verwoerd, 1975; Scholtz, 1985).

4. Structural analysis

4.1. Remote sensing analysis

A basic remote sensing study was used to carry out a preliminary structural analysis of the area, with a particular focus on the easily recognizable fractures that deform the NMP. Observations from remote sensing were subsequently ground-truthed during fieldwork (the main component of our study) and the results are presented in the next section.

Our simple remote sensing analysis is based on the study of a series of Landsat images (Fig. 5, RGB 742 spectral band composite, pan-sharpened to 14.25 m spatial resolution) and Google Earth imagery. Lineaments were mapped onscreen using the human eye without applying any minimum length rule. On the Landsat images one single illumination source is fixed to the NE, which can lead to interpretation bias wherein lineaments at high angle to the azimuth of the illumination source could be overemphasized (e.g. Smith and Wise, 2007).

However, the complete lack of vegetation, the excellent exposure conditions and the very high resolution of the Google Earth images made it possible to double check and improve the Landsat-based interpretation and generate a reliable lineament strike rose diagram.

Numerous laterally extensive and continuous linear features/lineaments, developed as a result of preferential erosion along steep to sub-vertical faults and fractures, can be mapped (Fig. 5; subsequent field work confirmed this interpretation). Indeed the NMP displays very prominent fractures and fracture sets characterized by systematic trends and consistent geometric relationships. The compilation of the strike orientation of several hundreds of lineaments (Fig. 5) reveals the relative narrow angular sector populated by the mapped strike directions and a stark predominance of NNW-SSE trends. The Namaqualand ductile grain, including lithological boundaries and the regional foliation, trends ca. E–W. There are numerous apparent E–W lineaments that follow this trend and that were not considered in our analysis as they represent lithological contacts or landforms entirely controlled by the foliation.

Based on their spatial arrangement, on their persistency and on the kinematic evidence that could be derived from the unambiguous displacement of visual markers, these structural features were grouped in four different systematic families of conjugate fractures.

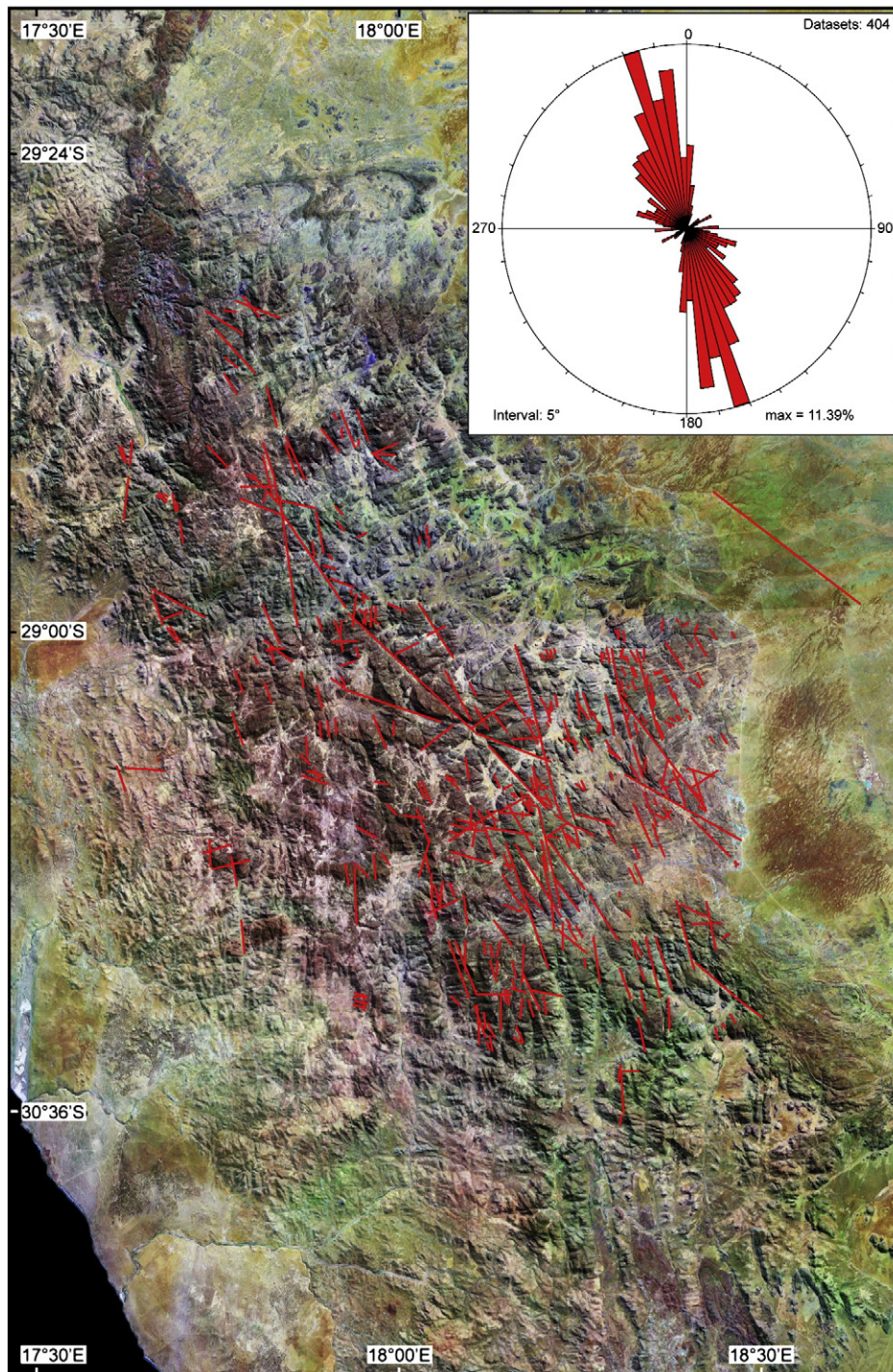


Fig. 5. Landsat image of the study area, focussed on the exhumed NMP. The latter is saturated of faults and fractures, which correspond to prominent sets of lineaments. The strike of more than 400 lineaments (red lines) is plotted in the rose diagram. (For interpretation of the references to color in this figure legend, the reader is referred to the web version of this article.)

A number of chosen examples are shown in Fig. 6. They are named here “a” to “d” and are sorted and characterized below according to the relative geochronological order that is described in detail in the discussion section of the paper. The rose diagram of Fig. 5 is moreover interpreted in Fig. 6 in terms of the strike angular dispersion of the faults of the four sets.

Set “a” This group is characterized by sub vertical conjugate fractures oriented from WNW-ESE to WSW-ENE and NW-SE, with sinistral and dextral kinematics, respectively. Their intersection

defines an acute angle bisected by a W/WNW-E/ESE-oriented greatest compressive horizontal stress direction - σ_1 (Fig. 6a and b). Fractures and faults are observed with variable length, from a few hundreds of meters to several kilometers. Although rarely seen at the mesoscopic scale in the field, set “a” includes some of the most impressive large lineaments of the region. One of them crosses the whole of the Namaqua highlands (it is easily visible in Fig. 5), strikes NW-SE and is almost 55 km long. It is interpreted as an originally sinistral fault belonging to a “giant” fault/fracture conjugate set.

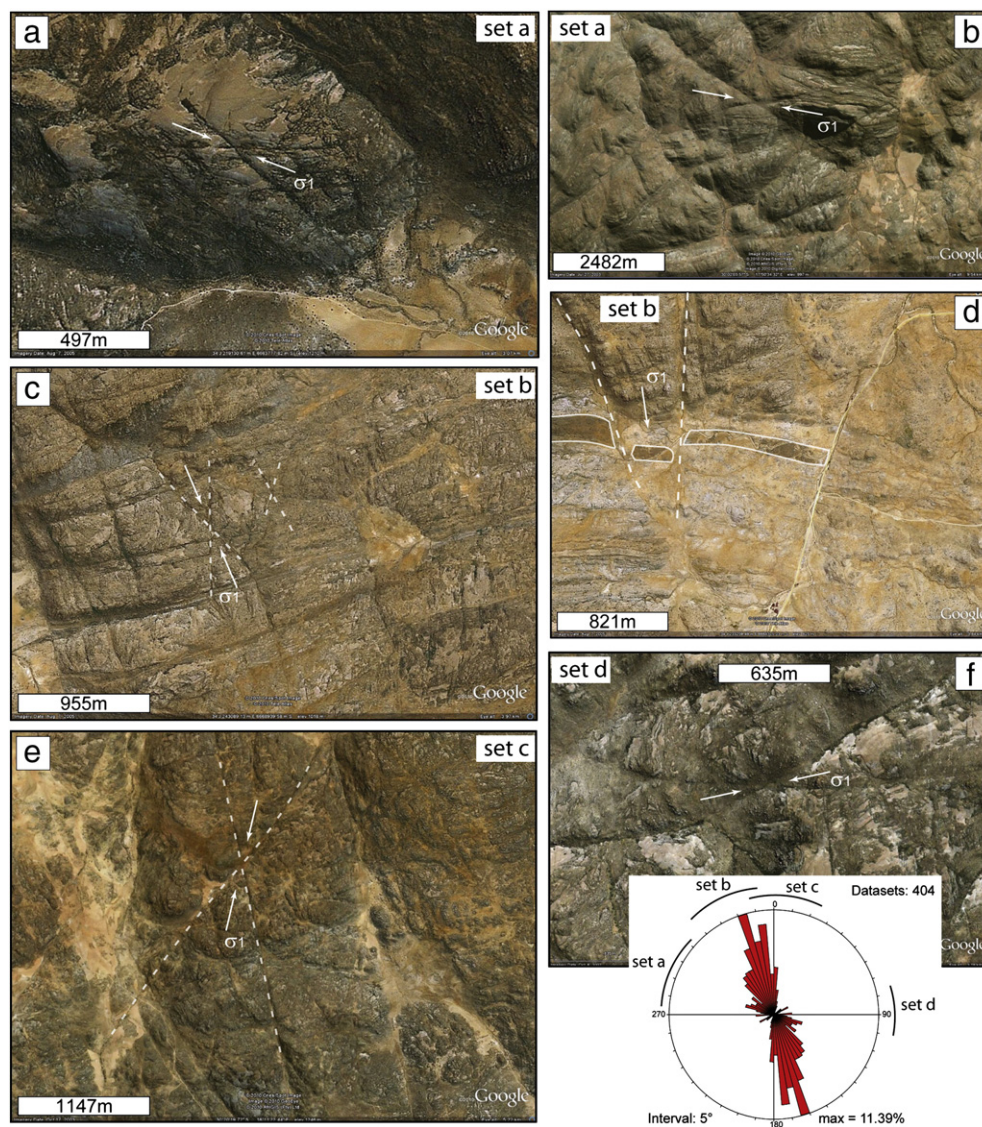


Fig. 6. Study of the high-resolution Google Earth images allowed the identification of 4 different systematic sets of conjugate faults/fractures (set “a” to set “d”). North up for all images.

Set “b” Faults and fractures that can be ascribed to this set are among the most common brittle structures of the entire NMP (Fig. 6c and d). They strike ca. NW-SE and N-S and their intersection defines an acute angle bisected by a greatest horizontal compressive stress oriented NNW-SSE. Fig. 6d confirms the unambiguous kinematics of this conjugate set, wherein a continuous, EW-trending dark lithological band is displaced by both NW-SE dextral and ca. N-S trending sinistral faults of set “b”.

Set “c” Conjugate sets of subvertical strike-slip fractures belonging to set “c” are only slightly misaligned with respect to faults of group “b” through a 20–30° clockwise rotation. Sinistral fractures strike approximately N-S, dextral ca. NE-SW. The greatest horizontal compressive stress derived from this set is thus oriented NNE-SSW (Fig. 6e). The geometric relationships between structural features of set “b” and “c” require significant reactivation of the ca. N-S-striking faults.

Set “d” Conjugate fracture sets belonging to group “d” are relatively small structures and are only rarely observed in the field. They define a W/WSW-E/ENE-oriented greatest compressive horizontal stress and their orientation, in places, is not far from that of faults and fractures assigned to set “a”, thus implying their possible reactivation (Fig. 6f). It cannot be

excluded, based on this simple analysis, that fractures of set “d” are actually slightly misoriented fractures of set “a”.

4.2. Field study results

Field structural investigations, including fault-slip data collection and analysis, were carried out on a number of conventional outcrops, polished pavements and trenches with the aim of establishing a robust and field-constrained model for the local brittle structural evolution. Fig. 7 shows examples of typical structures analyzed during our study. These are localized and discrete faults and their associated fault folds, shear and hybrid fractures, tension gashes and slickensided fault planes.

Specific attention was paid to direct crosscutting relationships among several generations of faults because this helped add constraints to the relative time sequence of events. Crosscutting relationships observed within the highly weathered silicified and kaolinitized mesas that cap the Namaqualand metamorphic rocks are, for example, shown in Fig. 8a; steep normal faults accommodating NE-SW extension consistently cut across and offset low-angle, top-to-the-NW and SE-dipping thrusts.

The analysis and characterization of fractures affecting lithologies of known age was used to bracket the age of deformation of specific

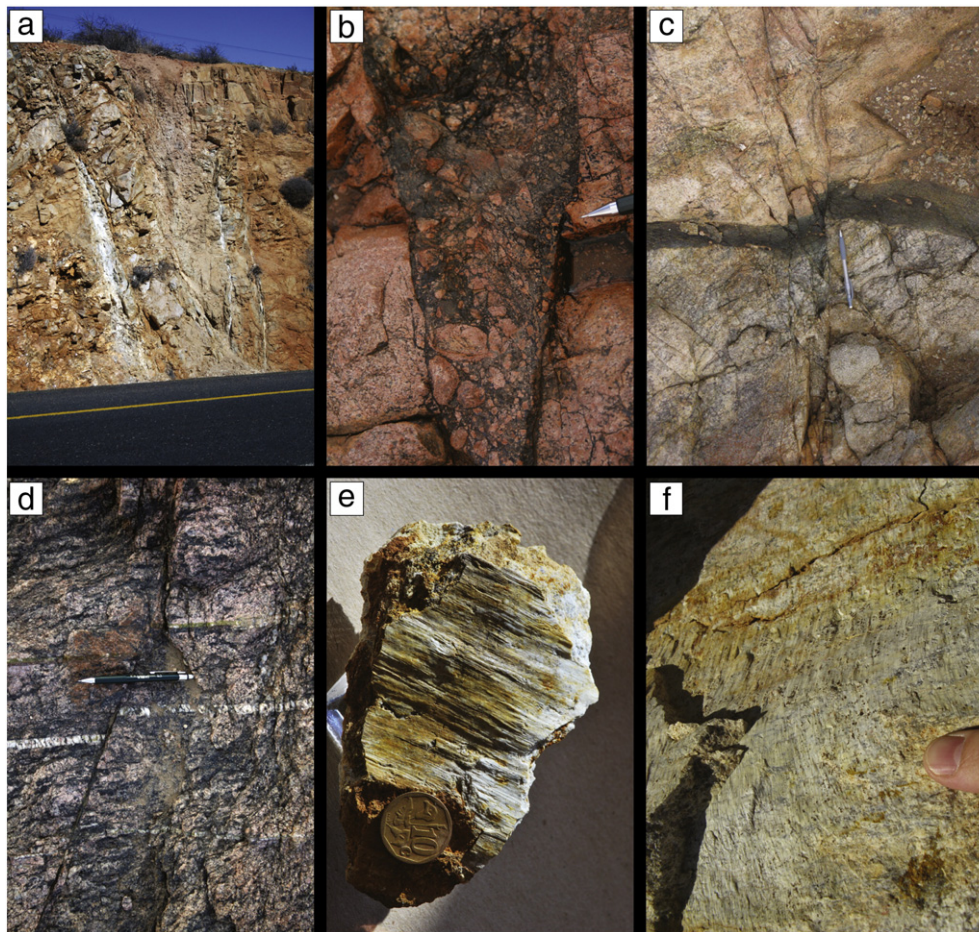


Fig. 7. Examples of brittle structural features investigated during this study. a): Discrete brittle transtensional fault (Loc. 20, Fig. 2; 29° 13.292', 17° 39.223'). b): Cataclasite formed at the expense of granite-gneiss of the Namaqua metamorphic complex (Loc. 55, Fig. 2; 30° 21.325', 18° 17.736'). The fault rock is associated with a sinistral brittle fault oriented N–S. c): Sinistral offset of a mafic schlieren within granite gneiss along a brittle deformation zone oriented 83/288 (same locality as b). d): Thin fracture oriented 88/066 causing centimetric sinistral offset of a quartz vein (Augrabies waterfalls; 28° 35.596', 20° 20.424'). e): Unoriented hand specimen of striated fault plane. f): Slightly curved striations along fault plane (Loc. 37, Fig. 2; 30° 07.316', 18° 27.244').

events. Fig. 8b, for example, shows the orientation of conjugate fractures mapped within Dwyka tillites, whereas Fig. 8c of sinistral faults cut by dextral faults and predating the emplacement of a volcanic plug of the Gamoep suite.

The implications of these geometric relationships used to generate the model and draw the conclusions of our paper are discussed below in detail.

4.2.1. Inversion of fault-slip data and fault-slip tendency analysis

4.2.1.1. Methodology. More than 300 fault-slip data were collected, processed and interpreted during this study to ground truth the structural observations derived through remote sensing, to place them in a consistent kinematic/geometric framework and to derive a robust model of the evolution of the stress field through time.

Collection of a fault-slip datum includes the fault plane orientation, the slip direction as determined by striations, and the sense of slip. The latter was established by conventional kinematic analysis of brittle structural features (e.g. Hancock, 1985; Petit, 1987). Inversion of fault slip data sets in terms of stress tensor relies on the Wallace–Bott hypothesis (Bott, 1959; Wallace, 1951) that states that the maximum resolved shear stress on a fault plane is parallel to the observed slip direction. A newly formed fault plane has an orientation that allows the relative magnitudes of shear stress τ and normal stress σ on this plane to meet with the Mohr–Coulomb yield criterion, $\tau = c + \mu\sigma$, where c is the shear strength and μ is the coefficient of friction.

According to these two mechanical laws, stress inversion techniques search for the state of stress that best accounts for a given fault-slip dataset by iteratively adjusting the theoretical slip pattern associated with a known stress state until it fits the slip pattern observed at the outcrop (e.g. Angelier, 1979; Angelier et al., 1982; Etchecopar et al., 1981). To this purpose, the orientation of the principal stress axes σ_1 , σ_2 and σ_3 , with $\sigma_1 \geq \sigma_2 \geq \sigma_3$ (compression positive) and the stress ratio $R = (\sigma_2 - \sigma_3) / (\sigma_1 - \sigma_3)$, which reflects the shape of the stress ellipsoid (oblate for $R > 0.5$; prolate for $R < 0.5$), are varied systematically so as to minimize the sum of all misfit angles with the misfit angle α , which represents the angle between the calculated maximum shear stress and the actual measured slip direction for an individual fault plane.

This approach derives kinematic (or strain) axes for each individual fault plane assuming that, during brittle deformation in upper crustal conditions, axes of strain coincide with axes of stress (e.g. Anderson, 1951). In this study, we used the numerical program 'TENSOR' (Delvaux and Sperner, 2003) to perform the stress inversion. The software computes the best fitting stress tensor for a given fault slip data set by an iterative procedure called "rotational optimization", by which the best solution is identified by rotating incrementally the computed stress tensor until optimization is attained with respect to the fault slip data set analyzed. A misfit function tends to (1) minimize the normal stress, (2) maximize the shear stress and (3) reduce the misfit angle α between the resolved shear stress and the real slip for each striated fault plane and thus controls the optimization procedure.

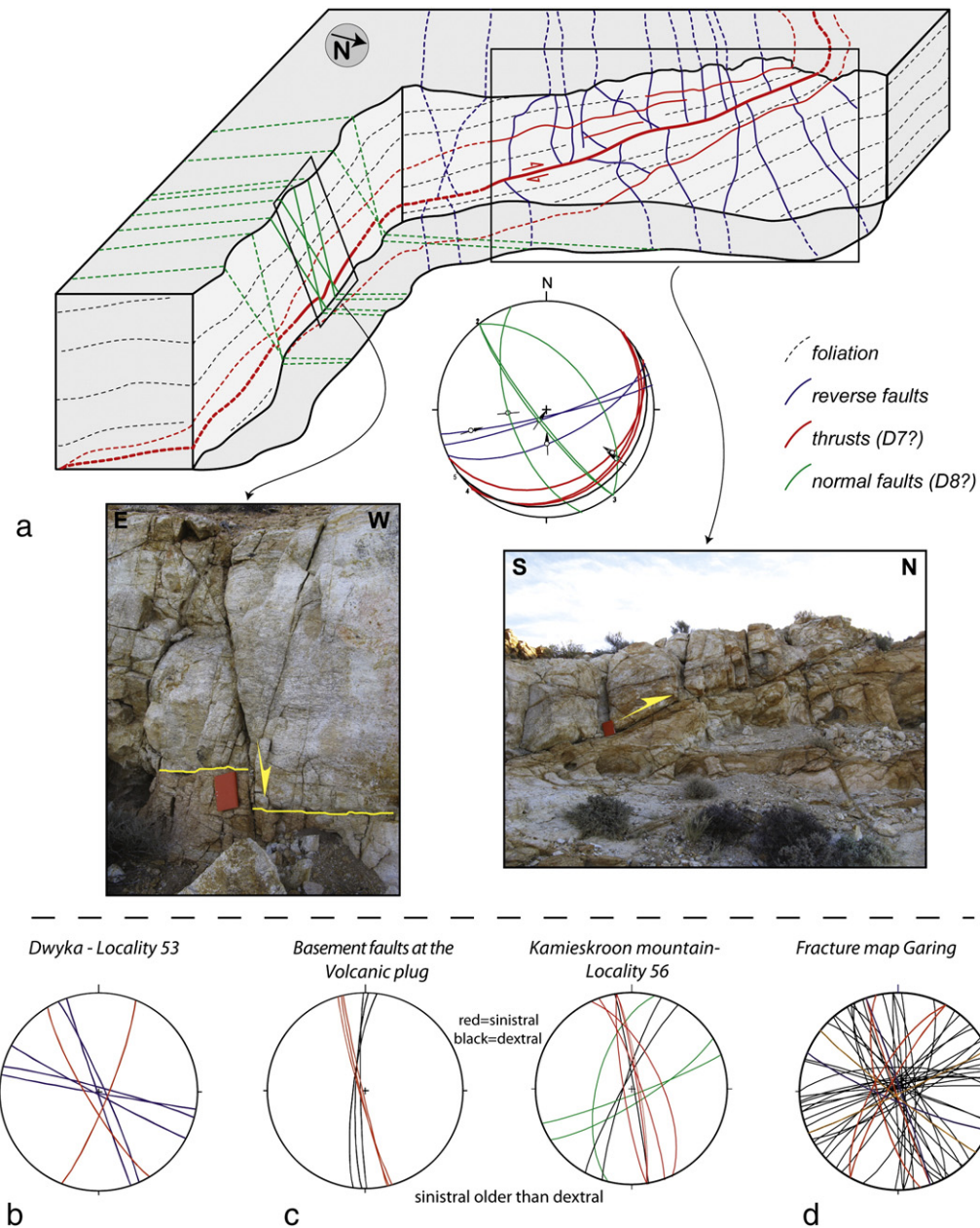


Fig. 8. a): Example of structural investigations at an outcrop of weathered metamorphic basement (Loc. 37, Fig. 2; 30° 07.316', 18° 27.244'). Systematic, mutual crosscutting relationships were documented, allowing the establishment of a relative time sequence of the faulting episodes. Deformation phase labels D7 and D8 refer to the scheme of Fig. 17. b): Conjugate fracture sets mapped within Permian Dwyka tillites (Loc. 53; Fig. 2; 30° 13.884', 18° 41.730'). c): Selected examples of dextral faults cutting across older sinistral faults. In the case of the Volcanic plug, sinistral and dextral faults are both cut by the intrusion. Green great circles plot conjugate fractures. d): Example of detailed outcrop fracture mapping at Garing (Fig. 2; 30° 06.128', 18° 29.941'). Conjugate sets are plotted by colored great circles. (For interpretation of the references to color in this figure legend, the reader is referred to the web version of this article.)

The quality of the final computed stress tensor reflects the number of data, their quality and the value of the misfit angle α (acceptable when $<30^\circ$). It is important to stress that no assumption is made on the attitude of fault planes relative to stress axes. Whether a fault plane is newly created or is instead a reactivated preexisting discontinuity has no consequence for the reconstruction of the reduced paleostress tensor. This is important in old basements because many fault movements have occurred along older fractures and inherited planar anisotropies.

Our methodological workflow relied on a preliminary manual sorting of the total data set. Inversion was then computed on the individual sub-sets, and the quality of the results was checked through the misfit criteria mentioned above. Fault slip data incompatible with a given stress tensor (for example because of misfit angle $\alpha > 30^\circ$)

were assigned to another sub-set or moved to the waste. The process was repeated until a unique and stable stress tensor was derived from a given, homogeneous sub-set.

In addition to the inversion of fault-slip data, in order to establish whether inherited faults within the NMP are critically stressed in the present-day stress field, we have carried out an assessment of fault slip tendency. The tendency of a specific fault to slip in a given state of stress can be estimated by the slip tendency parameter (T_S), defined as the ratio between shear (τ) and normal traction (σ_n) on a surface (Morris et al., 1996):

$$T_S = \frac{\tau}{\sigma_n} \quad (1)$$

Slip tendency is a useful expression of the frictional reactivation theory, which states that slip on a pre-existing and cohesionless surface takes place when the resolved shear traction exceeds friction. The calculated values can be normalized by the friction coefficient considered to represent failure conditions in a given setting. 0.6 is the value adopted in our analysis (Byerlee, 1978). For critically stressed fractures, normalized slip tendency values are equal or above unity whereas they are less than one for non-critically stressed fractures. The normal (σ_n) and shear (τ) tractions on any plane can be calculated by

$$\sigma_n = \sigma_1 l^2 + \sigma_2 m^2 + \sigma_3 n^2 \quad (2)$$

and

$$\tau = (\sigma_1 - \sigma_2)^2 l^2 m^2 + (\sigma_2 - \sigma_3)^2 m^2 n^2 + (\sigma_3 - \sigma_1)^2 l^2 n^2 \quad (3)$$

where l , m and n are the direction cosines of the plane normal in the principal coordinate system.

Slip tendency values can be calculated for all possible orientations by solving Eqs. (2) and (3) and substituting the results in Eq. (1). Final results can be then plotted in stereoplots, providing a quick and robust tool for assessing whether a specific orientation is critically stressed and has a high slip potential, both under dry and hydrostatic conditions.

4.2.1.2. Stress inversion results

Field data used in this study are presented in Figs. 9 and 10, with Fig. 9 showing individual outcrop raw data (see Fig. 2 for the localities). The dataset is complex and outcrops studied contain brittle features that are obviously the results of multiple faulting. Some of the sites investigated contain sufficient fault planes to allow the computation of individual, site-specific states of stress, but other sites contain statistically insufficient data (Fig. 9).

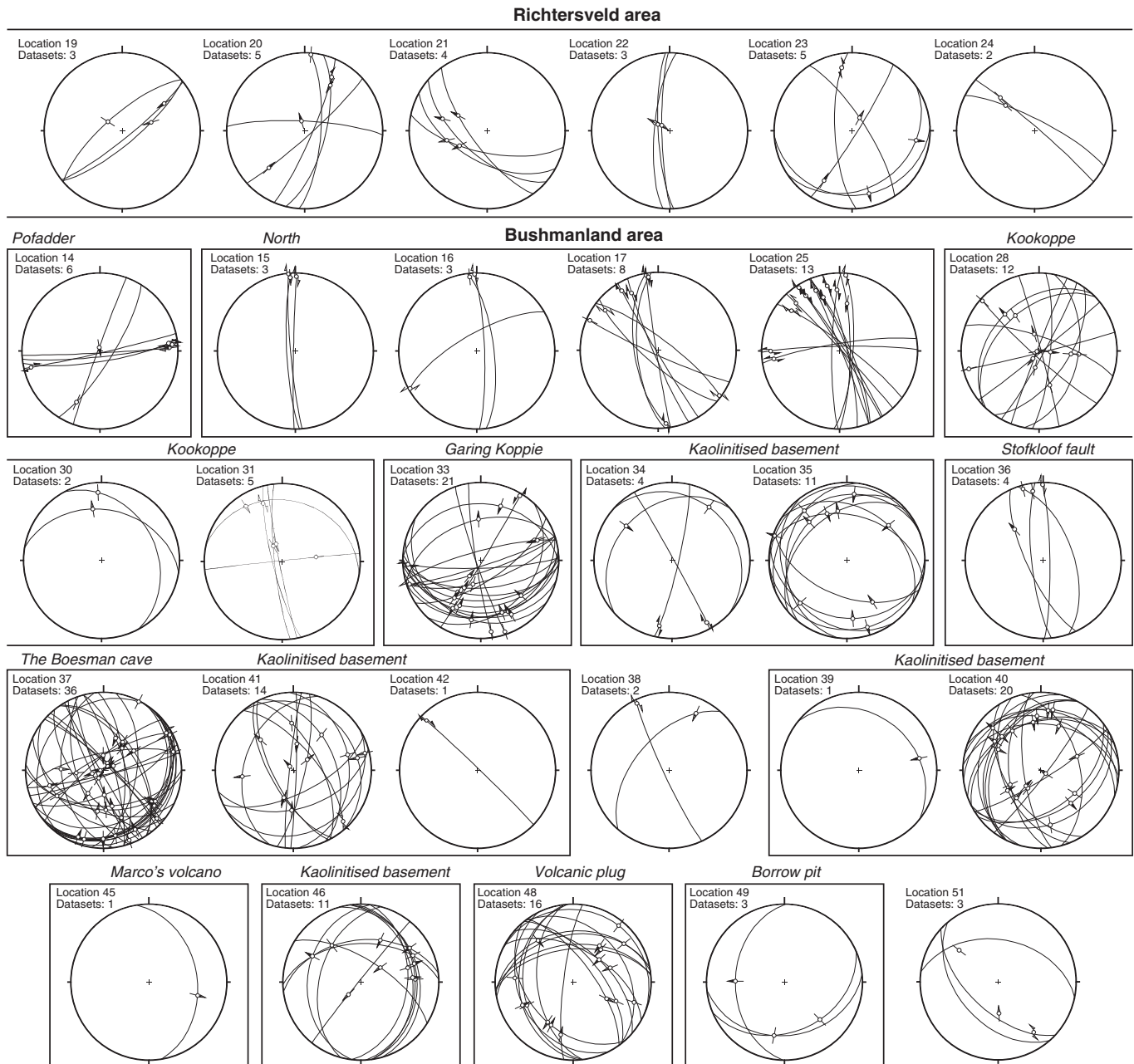


Fig. 9. Raw fault-slip data for the outcrops investigated in our study and located in Fig. 2.

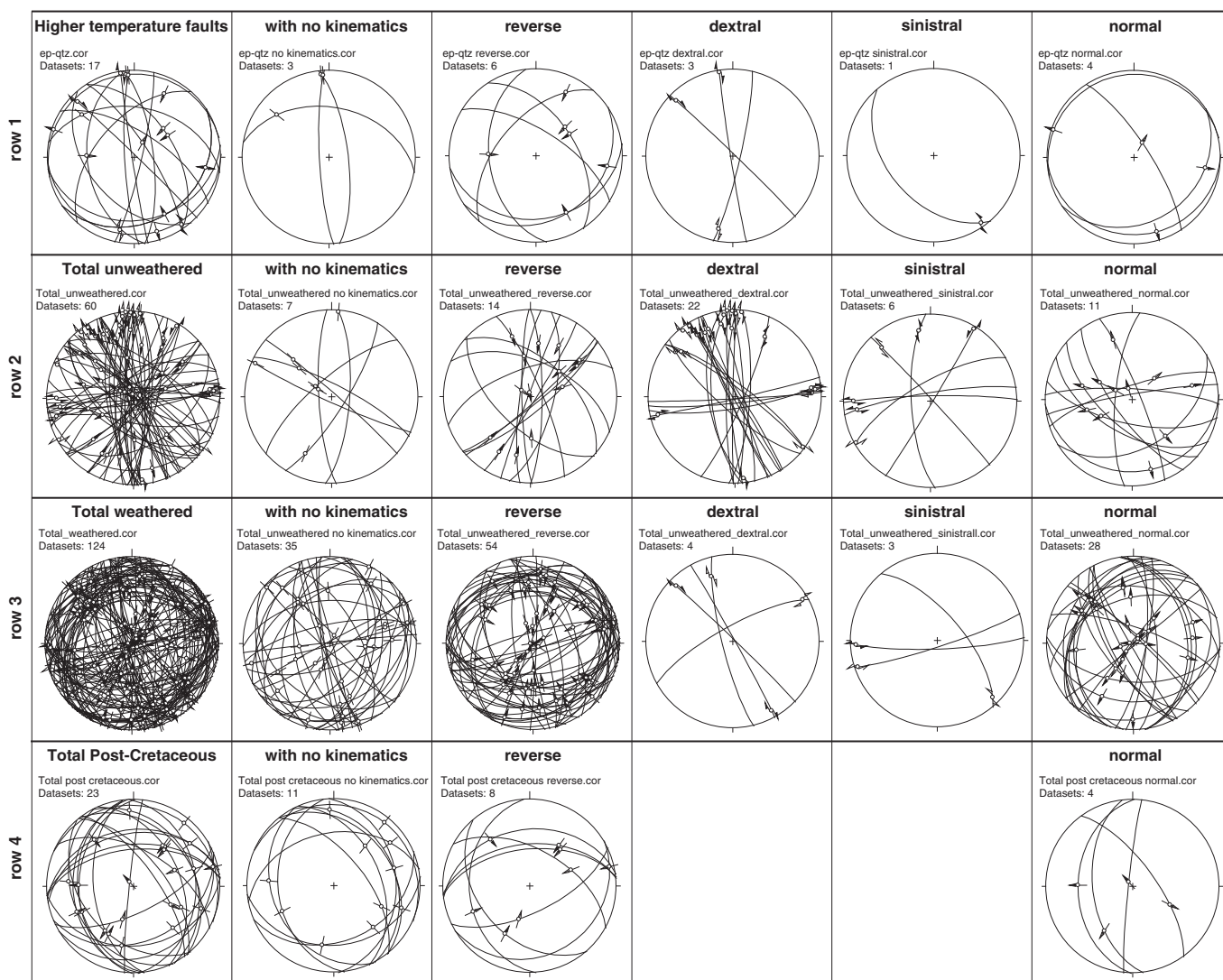


Fig. 10. Same data as in Fig. 9, but sorted according to the following four criteria, each of which corresponds to one row in the table: row 1: fault planes that are coated by relatively high-temperature mineral phases, such as quartz and epidote; row 2: fault-slip data derived exclusively from the fresh, unweathered Namaqua basement; row 3: fault-slip data derived from weathered sections of the Namaqua basement topping the mesas; row 4: fault-slip data derived from outcrops of post-(Late?) Cretaceous age. In detail, fault planes plotted in row 4 refer to volcanic breccias of the Gamoep suite.

Before meaningful inversion could be computed, it was necessary to separate the heterogeneous data sets into homogeneous sub-sets by using field criteria (for example age relationships or type of mineralization on the fault plane) and visual and mathematical compatibility criteria (e.g. grouping of calculated individual axes and maximum angular deviation of axes from calculated sub-set means). Fig. 10 shows the result of a preliminary conceptual sorting of the data wherein, given the common presence of the Late Cretaceous silicified and kaolinitized paleosols, of weathering profiles and alluvial fan sequence sediments of the Dasdap Formation that cap the Namaqua metamorphic rocks in the study area (Brandt et al., 2003), we have split the total fault-slip data into a batch derived from fresh NMP rocks (“Total unweathered”, row 2 in Fig. 10) from a second batch derived from the weathered sections, the paleosols and the fluvial sediments (“Total weathered”, row 3 in Fig. 10; see Fig. 3 for a schematic presentation of these relationships). In addition we used the Gamoep melilite suite as a second time marker during the sorting of our dataset. This approach is exemplified by the structural analysis of a ~20 m high, silicified, breccia pipe standing pillar-like above the basement granites SW of Vaalputs (Volcanic plug in Fig. 2). This explosive vent contains numerous striated fault planes (Location 48 in

Fig. 9) and was used to compute well-defined post-Late Cretaceous tensors.

The subset “Higher temperature faults” (row 1 in Fig. 10) refers instead to striated fault planes decorated predominantly by relatively high-temperature mineral phases such as quartz and epidote (e.g. Drake et al., 2009). These were used to make inferences about the earlier part of the brittle deformational history of the area, assuming that this took place at deeper crustal conditions than the younger events.

Based on the assumption that faults that deform the unweathered NMP but not the paleosols result from a history predating the Late Cretaceous development of the latter, we processed initially fault-slip data merged from the “Higher temperature faults” and “Total unweathered” subsets (data from row 1 and 2 in Fig. 10), implying that these are the oldest brittle features documentable by our study. Most of these striated fault planes are steep to vertical strike-slip faults and bear subhorizontal striations. The corresponding total dataset is complex and heterogeneous and it contains faults that formed in response to more than just one single deformation phase. Four distinct and relatively robust compressive paleostress tensors were derived and are labeled 1 to 4 in Fig. 11. In addition, there are

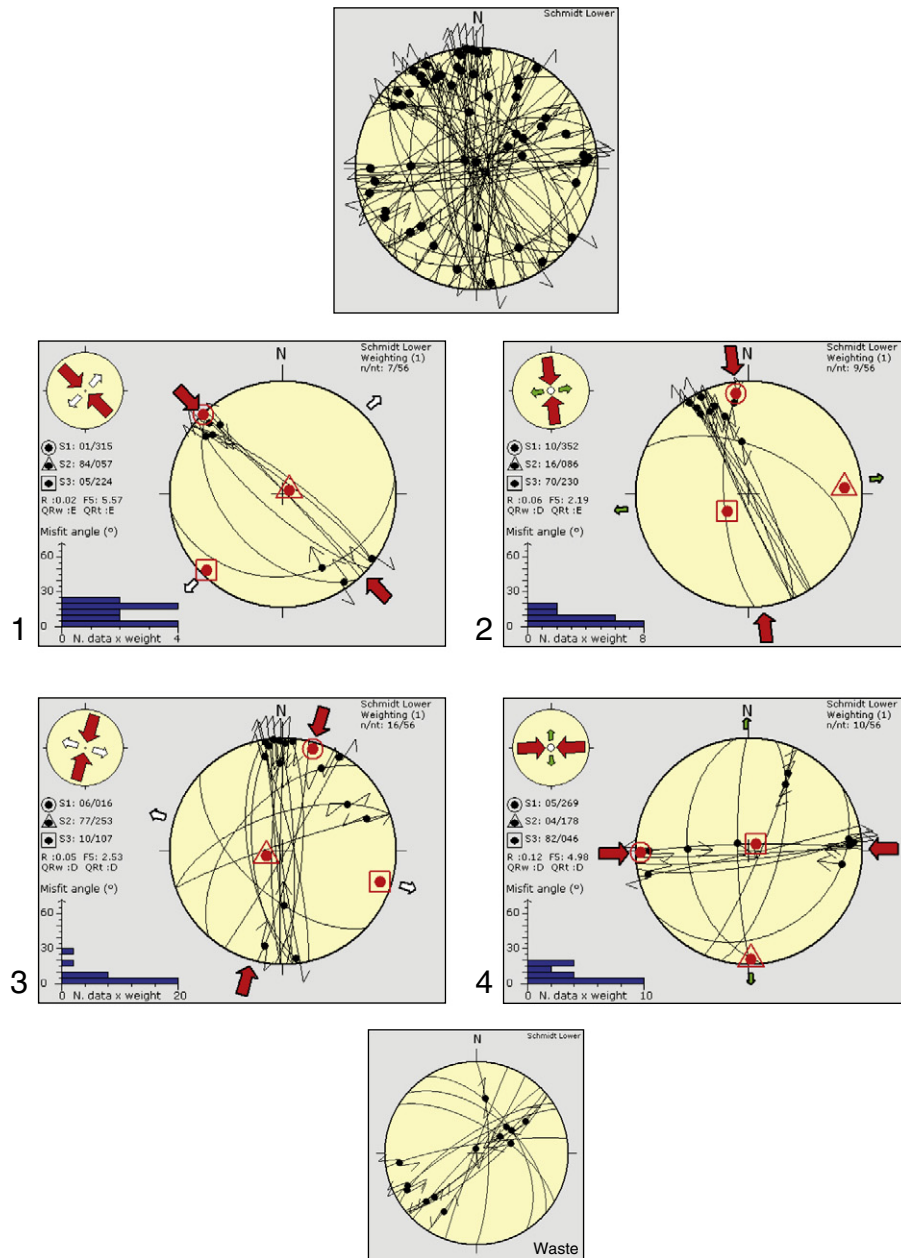


Fig. 11. Compressional paleostress tensors derived from the fault-slip data of rows 1 and 2 in Fig. 10. Stress tensors are labeled 1 to 4 for ease of reference. See text for more details.

a number of normal and strike-slip faults (Fig. 10), which were used to constrain two additional states of stress (Fig. 12).

Tensors 1 to 4 are all based on the inversion of sets of conjugate, steep shear fractures, which show variable degrees of preservation (Fig. 11). Paleostress Tensor 1 is characterized by broadly overlapping sinistral and dextral strike-slip sub-vertical fault planes trending NW-SE. These do not define a clear conjugate set, but a reliable strike-slip stress tensor was computed with a sub-horizontal σ_1 oriented 01/315 and σ_3 at 05/224. Caution is necessary when interpreting this tensor and a few more of those discussed below (e.g. Tensor 4), as the acute angle defined by the faults of the suggested conjugate set is extremely tight and some of the faults are subparallel to σ_1 (mechanically unlikely). Similar results were however obtained also by Viola et al. (2009), Saintot et al. (2011) and Viola et al. (2011) in studies dealing with the Precambrian basement of SW Scandinavia, which is fully saturated with fractures and which, similarly to the Namaqualand basement, underwent a long and complex brittle history.

Under these conditions it is common to observe rather “closed” conjugate sets, which likely reflect low friction coefficients and severe reactivation. These factors can indeed promote slip along highly misoriented fault planes.

Stress Tensor 2 is defined by a statistically robust set of NNW-striking dextral and a few N-S sinistral strike-slip faults. A tight acute angle constrains σ_1 at 10/352 and a sub-vertical σ_3 at 70/230.

Stress Tensor 3 suggests a minor clockwise rotation of the greatest compressive stress σ_1 with respect to Tensor 2, with σ_1 oriented 06/016. A well-defined family of N-S-trending sub-vertical dextral faults and a set of ca. NE-SW sinistral faults characterize it. We interpret these two tensors as truly representative of two separate and distinct shortening episodes with an only slightly different σ_1 (and not as just resulting from data scatter and possible interchange of σ_2 and σ_3) because several outcrops presented compelling evidence of initially sinistral c. N-S trending faults that were reactivated dextrally, consistent with a progressive clockwise reorientation of σ_1 .

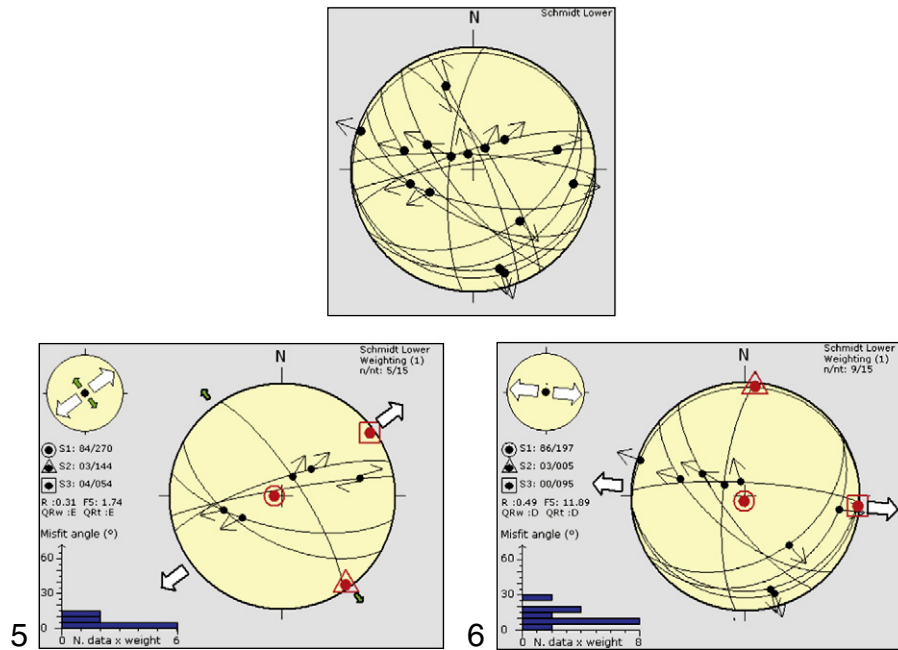


Fig. 12. Extensional paleostress tensors computed from the fault-slip data of rows 1 and 2 in Fig. 10.

The last compressive tensor derived from these faults, *Tensor 4*, constrains a ca. E–W σ_1 at 05/269 and a sub-vertical σ_3 at 82/046.

The “waste” of this analysis consists of 13 faults that do not fit the above tensors, because of either geometric or kinematic incompatibility (Fig. 11).

Several normal faults were also found (Fig. 10) and have been used to compute two different tensional stress tensors (Fig. 12).

Tensor 5 was computed by inverting steep (probably reactivated older strike-slip fault planes) transtensional faults and is defined by a sub-horizontal extension direction toward 054 (Fig. 12). The second tensional tensor (*Tensor 6*) yields a ca. E–W horizontal extension direction (Fig. 12).

Processing of fault-slip data from the weathered silicified and kaolinitized mesas and from the Dasdap Formation yielded 2 compressive (Fig. 13) and 2 tensional (Fig. 14) paleostress tensors, all of which are taken to postdate those described hitherto. In order to test the possibility of partial reactivation of preexisting faults, which are those that in our work-flow predate the Late Cretaceous, the deposition of the Dasdap Formation and the development of the paleosols, we have tested the compatibility of the “waste” from the previous analysis (that is, from the computation of *Tensors 1* to 6) with the tensors derived from the “Total weathered” dataset. Results were positive, given that all but one of the 13 rejected faults could be implemented successfully within the sub-sets inverted to *Tensors 7* to 10.

A first tensor (*Tensor 7*, Fig. 13) was generated through the inversion of a set of ca. NW- and SE-moderately dipping thrusts. σ_1 trends NW-SE and is horizontal (00/307), with a sub vertical σ_3 oriented 86/211. The stress ratio of 0.4 indicates thrusting under almost pure compression conditions.

A second, shortening tensor (*Tensor 8*, Fig. 13) was derived through the inversion of a set of NW-SE to E–W striking and moderately dipping thrusts and several sub vertical strike-slip faults taken from the waste of the “Total unweathered” subset. A horizontal σ_1 striking 00/207 was obtained, together with a sub vertical σ_3 at 84/111. The corresponding stress ratio of 0.75 indicates radial compression.

In addition, two clear and statistically robust extensional stress tensors were constrained by a number of normal faults (*Tensor 9*

and 10, Fig. 14). *Tensor 9* constrains extension along the direction 08/048, and is characterized by a stress ratio of 0.25. *Tensor 10*, on the other hand, defines an almost orthogonal stretching direction, wherein σ_3 is now oriented 02/292 and the stress ratio is 0.31.

In the analysis of the post-Late Cretaceous stress tensors, data shown in row 4 of Fig. 10 deserve special attention. Those striated fault planes are derived predominantly from a volcanic breccia pipe that belongs to the Gamoep suite (*Volcanic plug* in Fig. 2). Apart from a few extensional faults that do not allow any statistically reliable inversion, striated planes derived from this “well-dated” time marker confirm a robust compressional stress tensor with a σ_1 oriented 09/230 (Fig. 15). This is similar to the shortening direction 00/207 mentioned above (*Tensor 8* of Fig. 13), which, in the absence of more compelling and geochronologically-constrained evidence, justifies the merging of the data derived from the silicified and kaolinitized paleosols and from the Dasdap Formation with the data from the volcanic plug.

4.2.1.3. Slip tendency analysis results

Overcoring data from Namaqualand mines indicate that the region is presently in a state of strike-slip faulting regime, with an overall NW-SE oriented compression (Nieuwoudt and Rozendaal, 1990). σ_1 values range from 56 MPa at 720 m depth to 83 MPa at 1572 m depth, and σ_3 values from 17 MPa to 36 MPa, respectively. σ_2 is invariably subvertical. Stress ratios $R = (\sigma_2 - \sigma_3) / (\sigma_1 - \sigma_3)$ vary generally between 0.1 and 0.2 (Fig. 16a). The stress state evolution with depth is shown in a differential stress vs. mean stress diagram (Fig. 16a for dry conditions and Fig. 16b for the case of presence of water under hydrostatic conditions), together with Mohr-Coulomb failure curves for friction coefficient values (μ) of 0.2, 0.4, 0.6 and 1.0. The data from various depths indicate that the stress state is rather close to the failure curve with friction coefficient 0.6, which is typically considered as the limit for frictional reactivation (Byerlee, 1978).

5. Discussion

The goal of our study is to propose a scheme for the regional brittle evolution, wherein each computed paleostress tensors is placed in

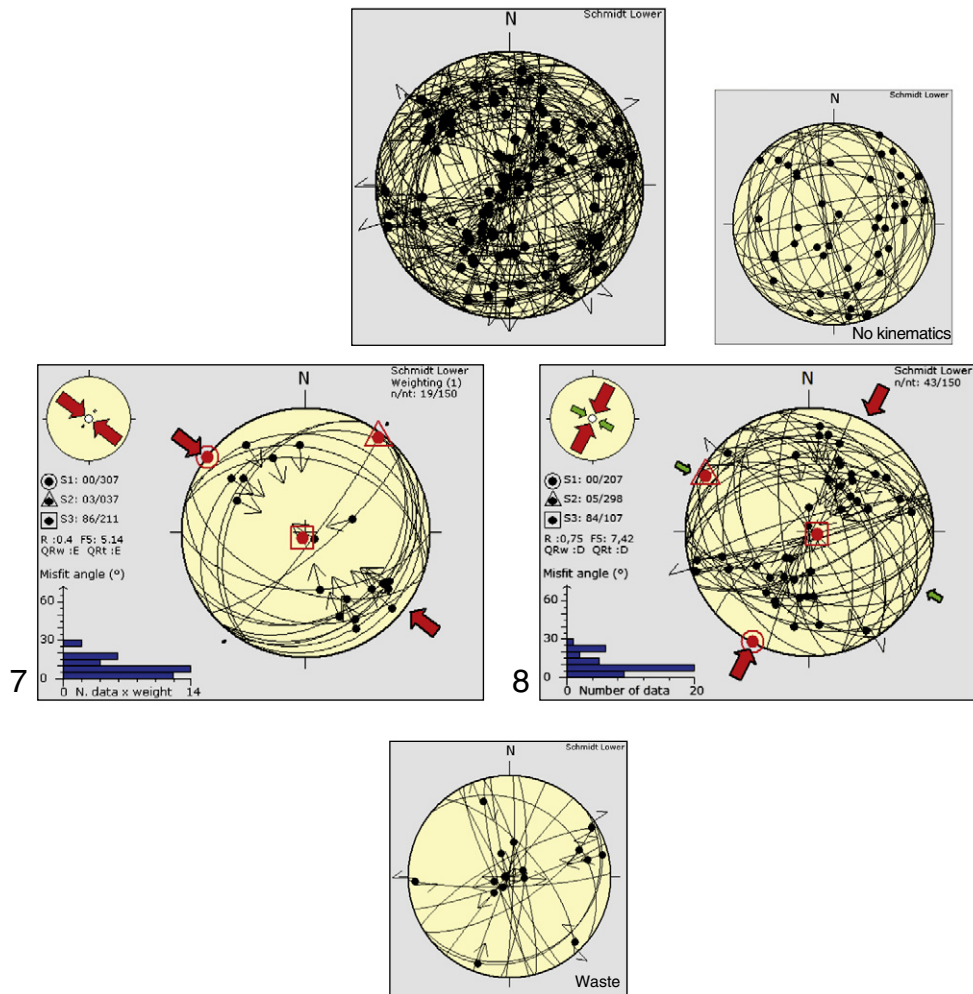


Fig. 13. Compressive paleostress tensors obtained from the inversion of fault-slip data from the weathered silicified and kaolinitized mesas and from the Dasdap Formation (row 3 in Fig. 10).

time and assigned to one of the orogenic events that have affected the region. It is important to stress that studies of this kind rely on a number of assumptions and that the complex and long geological evolution of the region makes any analysis of the brittle history extremely challenging. As a consequence, it should be born in mind that there are several sources of uncertainty involved in our study and that the results and the model presented below should be evaluated critically and cross-checked against other types of independent observations.

Fig. 17 is a “paleostress tensor vs. time” chart, with which we suggest a conceptual model for the evolution of the region. The paucity of well-dated time markers and the lack of geochronological data to better constrain the time dimension of our stress tensors unfortunately compromise the establishment of an absolute time-sequence of deformational events. Nonetheless, the time line is punctuated by a few, broadly defined “episodes”, which can be used to frame the states of stress into narrower time windows. In addition to the Late Cretaceous paleosols, the Dasdap Formation (Brandt et al., 2003) and the Gamoep melilite suite, we can also rely on one important and well constrained Mid Cretaceous tectonic event related to margin uplift and a pulse of accelerated denudation along the Southern Africa margin (e.g., Brown et al., 2000; Kounov et al., 2009; Tinker et al., 2008). To refine our reconstruction, we have also reviewed a significant amount of literature that deals with the state of stress of the African plate during its evolution. Fig. 18 presents a comprehensive compilation of the relevant literature; the figure allows a synthetic overview

of the main compressive and extensional episodes recognized or suggested hitherto for various parts of the African plate (e.g. Basson and Viola, 2003, 2004; Davies and Coward, 1982; Frimmel, 2000; Gresse, 1995; Guiraud and Bosworth, 1997; Haddon and McCarthy, 2005; Johnston, 2000; Kounov et al., 2009; Nürnberg and Müller, 1991; Raab et al., 2002; Rabinovich and LaBrecque, 1979; von Veh, 1993).

In synthesis, our model is derived through the comparative analysis of our own results against the available time markers and the known episodes of crustal compression and extension. We discuss this model below in detail, from old to young.

5.1. Pan African history

The brittle deformational history we have investigated began probably already by ca. 0.95 Ga in response to the exhumation and progressive cooling of the rocks of the Namaqua Belt (Cornell et al., 2006; Eglington, 2006; Frimmel and Frank, 1998). The Pan African orogenic cycle, which resulted in the amalgamation of the supercontinent Gondwana (e.g. Unrug, 1997), was expressed in southwest Africa by the development of the Gariep Belt (Fig. 1) and its subsequent accretion onto the Namaqua foreland (e.g. Frimmel, 2000). Docking caused an important brittle structural overprint of the Namaqua foreland, whereas only minor thermal resetting is instead reported, mostly confined to the most proximal part of Namaqualand foreland and to discrete zones (Frimmel and Frank, 1998). Existing models for the buildup of the Gariep Belt (e.g. Frimmel, 2000; Gresse, 1994, 1995)

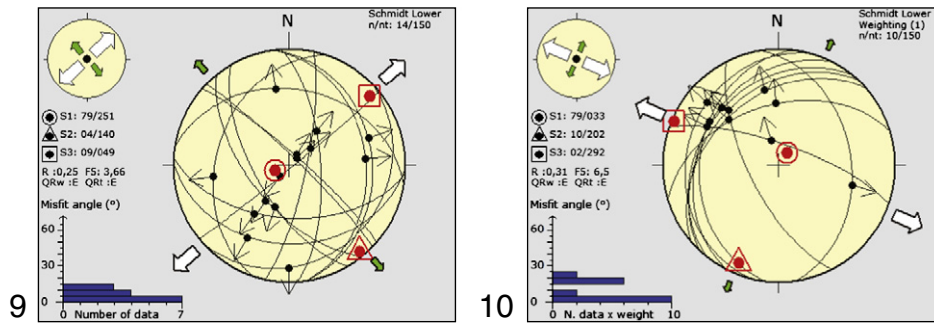


Fig. 14. Extensional paleostress tensors computed from the fault-slip data of row 3 in Fig. 10, that is from the weathered silicified and kaolinitized mesas and from the Dasdap Formation.

agree in suggesting a progressive reorientation of the principal shortening direction during orogenic evolution as well as significant strain partitioning due to the shape of the curved Gariep Arc. Frimmel (2000; his Fig. 4), for example, has proposed that the evolution of the Pan-African syn-orogenic stress field began with an overall E–W compression at about 580–540 Ma, followed by sinistral transpression resulting from ca. NW–SE shortening and followed by a later phase of NE–SW directed compression in the southern part of the belt at about 490–500 Ma. Gresse (1994) elaborated on the structural mapping by von Veh (1988, 1993) and Davies and Coward (1982) and in addition reported a late phase of ca. easterly-vergent thrusts and asymmetric folds along the southernmost part of the Gariep Arc exposed onshore. All authors concur on significant strain partitioning along strike and variable kinematics. These reconstructions are all based on the analysis of structures within the belt itself, but no structural analysis was carried out in its foreland (that is, Namaqualand).

Our results help bridge this gap. We suggest that the earliest mappable brittle structural features of western Namaqualand can indeed be ascribed to the waning stage of the Pan African evolution and the docking of the Gariep Belt. The structures considered as representative of this event are striated faults planes and fractures that affect the unweathered parts of the basement and are coated by quartz and

epidote, indicative of relatively high T conditions (e.g. Drake et al., 2009). These do not continue into the stratigraphically higher Late Cretaceous weathered mesas or are geometrically and kinematically incompatible with the tensors derived from fault-slip data measured within the mesas and the Late Cretaceous rocks. In our reconstruction, we therefore assign paleostress Tensors 1 to 4 (Fig. 11) to the late Pan-African event (no other significant regional sources of proximal or far-field stresses are known to have affected the region between the assembly of Gondwana and the initiation of its dispersal) and identify 4 separate shortening phases, D1 to D4 (Fig. 17) for the Namaqualand foreland. We interpret them as resulting from the accommodation of far-field stresses in a foreland crustal block that, due to its partial exhumation, had already attained thermal conditions leading to its overall brittle behavior.

The establishment of a relative chronological sequence for the events from D1 to D4 is not straightforward. However, based on the comparison with the sequence of deformational episodes proposed for the “indenting” Gariep Belt, we propose the scheme of Fig. 17. D1 is interpreted as the oldest shortening phase because of limited evidence of reactivation and because of its overall geometric compatibility with the earliest shortening by Frimmel (2000). As mentioned earlier, we assign to D1 one of the largest and most significant faults

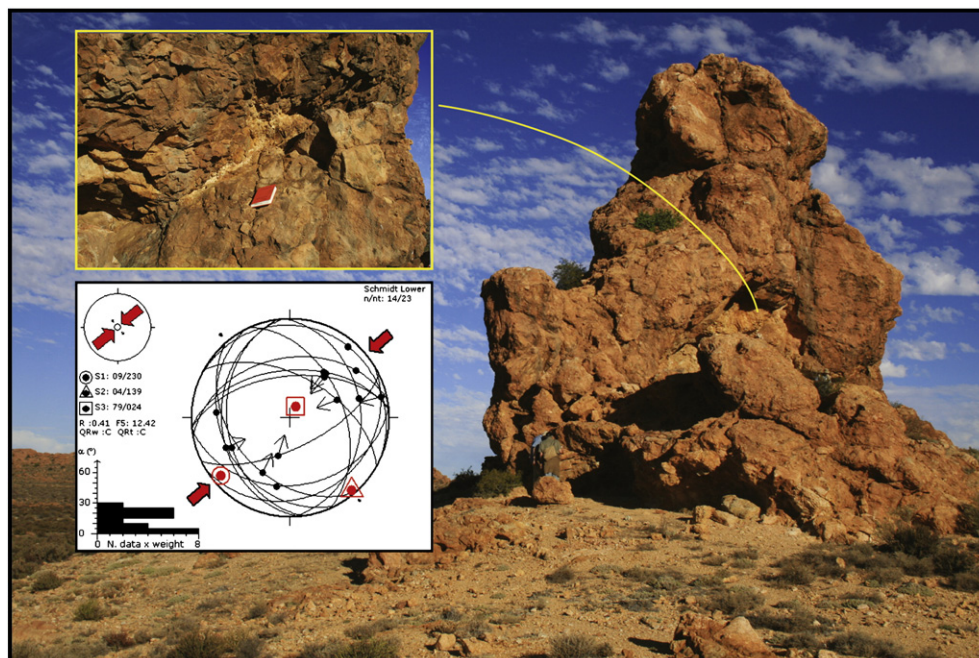


Fig. 15. View to the north of a c. 20 m high, silicified, breccia pipe standing pillar-like above the Namaqualand basement granites. The breccia is internally faulted as shown in the detail photograph. Stress inversion indicates a well constrained NE–SW phase of shortening.

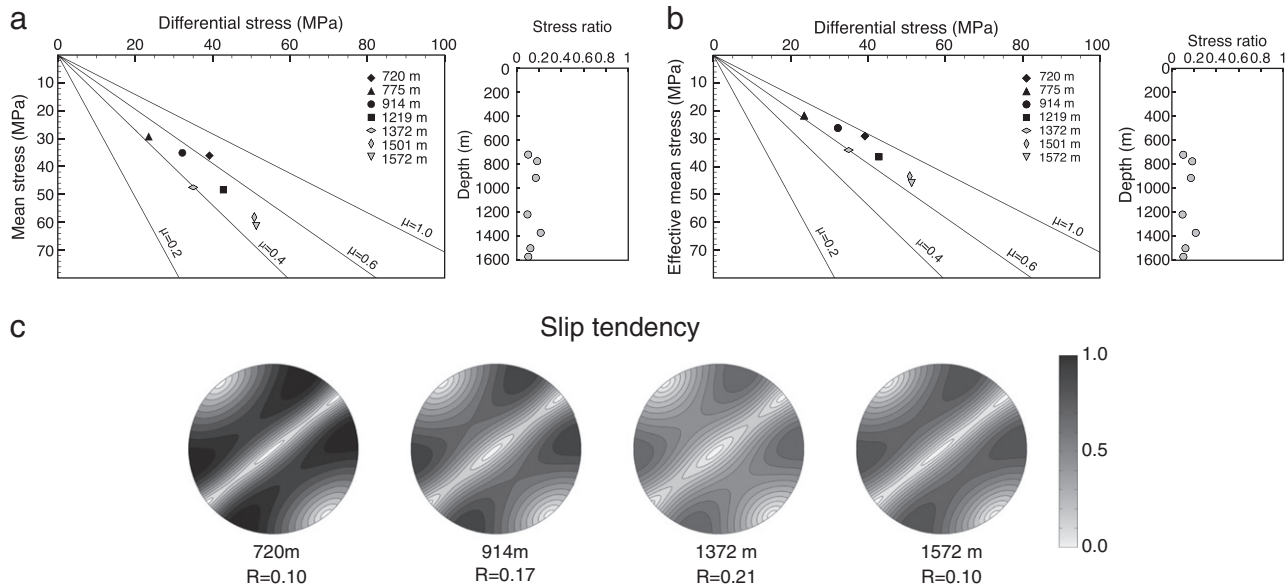


Fig. 16. a): Differential stress vs. mean stress diagram of the stress measurements from various depths at Namaqualand for a dry system. b): Results for the case of water under hydrostatic conditions. In both cases, Mohr-Coulomb failure curves are shown for friction coefficient values (μ) of 0.2, 0.4, 0.6 and 1.0. Stress ratio values at various depths are also shown. c): Slip tendency plots calculated for the present day stress state in Namaqualand, for different depths. Slip tendency values of 1 indicate that the specific orientation is close to failure at the given stress state. Lower hemisphere, equal area projections.

that dissect the Namaqua basement of the region studied (Fig. 4). The common observation in the field of convincing evidence of fault reactivation consistent with a progressive clockwise rotation of the greatest compressive stress from its initial ca. NW-SE trend is in agreement with our reconstruction and D2 and D3. For example, several cases of dextral reactivation of ca. N-S trending and originally sinistral faults have been documented (Fig. 7c), consistent with the transition from D2 to D3 (Fig. 17). Structures formed during D2 and D3 are the most common and form a dense fault network that affects the entire Namaqualand (Fig. 4). It is not clear at this stage whether these are two separated events, or instead the expression of a progressive rotation of the greatest compressive stress. Structures that can be assigned to D4 are not so numerous and are found predominantly within the northernmost part of the study area.

Results of the fault-slip data inversion procedure find support in the remote sensing analysis. Shortening directions almost identical to those constrained by the paleostress tensors characteristic of deformation phases D1-D4 were in fact inferred through the analysis of the imagery of the region (Fig. 6), which has led to the identification of four systematic sets of conjugate strike-slip faults (set “a” to set “d” of Fig. 6). We propose that fault sets “a”, “b”, “c” and “d” are the result of deformation phases D1, D2, D3 and D4, respectively. The subvertical planar attitude of the faults that we assign to sets “a” to “d” explains why they were picked selectively by the remote sensing analysis. Most of the faults and fractures of the later tectonic events are either the result of reactivation of these Pan African precursors or are simply not seen as straight (and easily recognizable) lineaments on the remote sensing imagery due to their low dip (see below).

5.2. Early to Mid Cretaceous evolution

The first extensional paleostress tensor derived from the “Total unweathered” dataset (data of row 2 in Fig. 10 and Tensor 5 in Fig. 12) is tentatively assigned to the Late Jurassic–Early Cretaceous stage of the opening of the South Atlantic Ocean (D5 in Fig. 16; Rabinovich and LaBrecque, 1979; Nürnberg and Müller, 1991). Striated fault planes inverted to compute it were mapped mostly along a cross-section from Springbok to the coast, thus at high angle to the present coastline.

Numerous brittle faults occur (e.g. Fig. 7a) but many do not show clear kinematic evidence. Only a few fault planes could therefore be used to constrain these directions; nonetheless, we believe that the computed tensor is geologically meaningful. For example, the NE-SW extension direction we propose is mechanically compatible with the general NW-SE to WNW-ESE strike direction of Early Cretaceous doleritic dikes, such as the Cape, the Mehlberg and the Garies-Knersvlakte dyke swarms, dated at about ca. 134–132 Ma (Reid and Rex, 1994; Fig. 2) and widely acknowledged as reliable strain gouges of the initial crustal stretching linked with the opening of the South Atlantic.

It is intriguing, however, that one of the most important tectonic events to have affected the western margin of the African continent during the Mesozoic is expressed in our study by only a handful of striated fault planes (only 5 faults were inverted to constrain this extensional event; Fig. 16). It should be kept in mind, though, that the study area formed a domain of the passive margin that remained rather distal from the actively rifting area. Most of the more intensively faulted and stretched margin is presently part of the submerged African shelf, not the target of our study. Moreover, the paucity of extensional structures in the study area that can be ascribed to this stage of the opening of the Atlantic Ocean is consistent with the absence of faults causing offset across obvious lithological/strain markers such as the Neoproterozoic Gannakouriep dyke swarm (Fig. 2).

In fact, far-field, Early Cretaceous NNE-SSW extensional stresses were proposed by Basson and Viola (2003, 2004) for the core of the Kaapval craton of South Africa (thus far away from the actively deforming Atlantic passive margin) based on studies dealing with the emplacement mechanisms of Early Cretaceous kimberlitic dykes (Fig. 18). They proposed a tectonic scenario wherein tensional stresses generated by the incipient break-up and heralded by the transcurrent Agulhas-Falkland fracture zone, led to localized crustal extension within the continental interior in the brittle (seismic) carapace of the upper crust triggering the formation of kimberlite dyke-fracture arrays.

The second, ca. E–W oriented extensional stress tensor (D6 in Fig. 17) is interpreted as being connected with the significant, tectonically induced Mid Cretaceous (115–90 Ma) denudation episode that has been inferred to be responsible for the removal of up to 2.5–

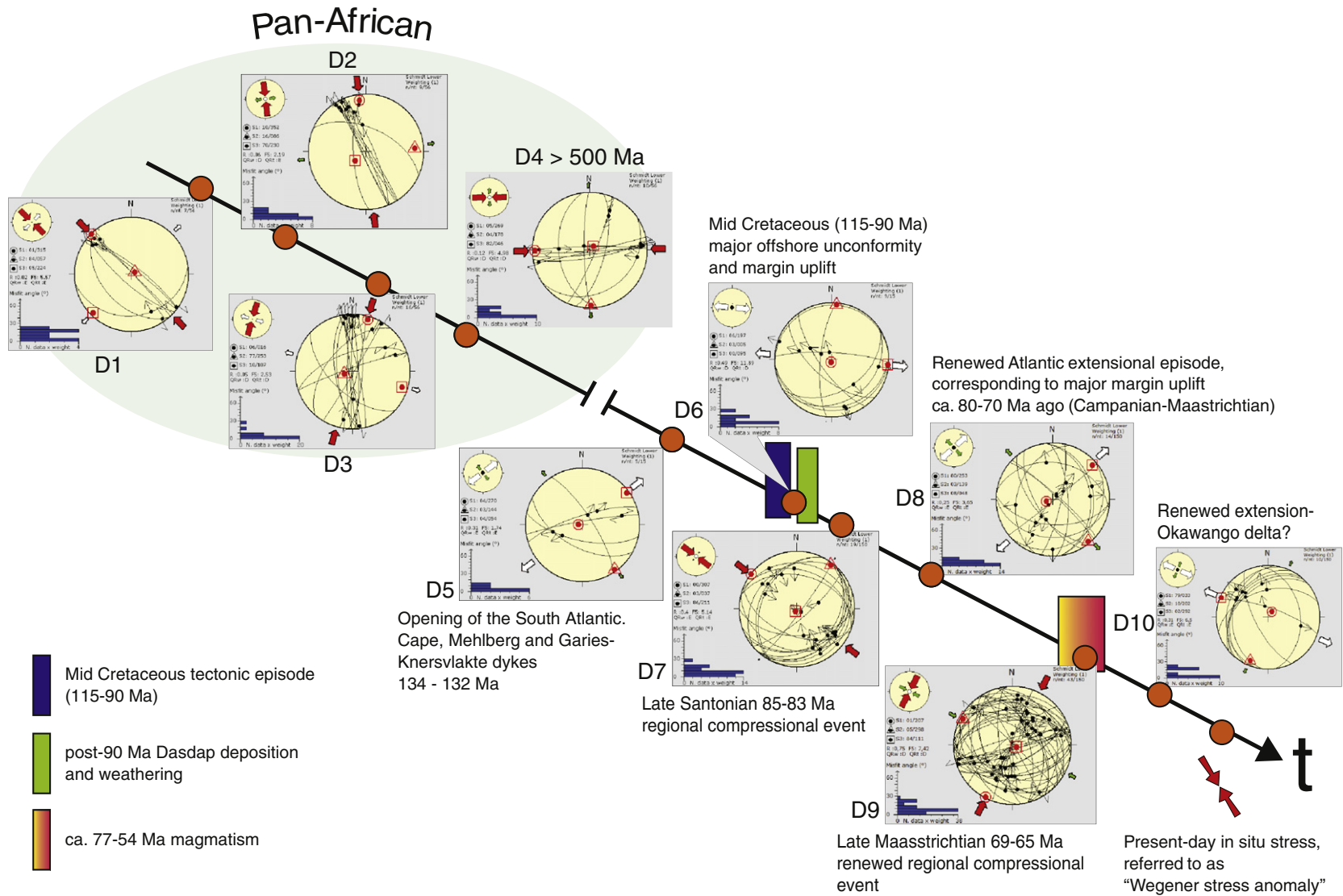


Fig. 17. Conceptual model of the brittle evolution of Namaqualand from the late stages of the Pan-African orogenic cycle to present-day. The time line is punctuated by geological events that are known to have affected the region and that are used to constrain the sequence of the states of paleostress derived in our study.

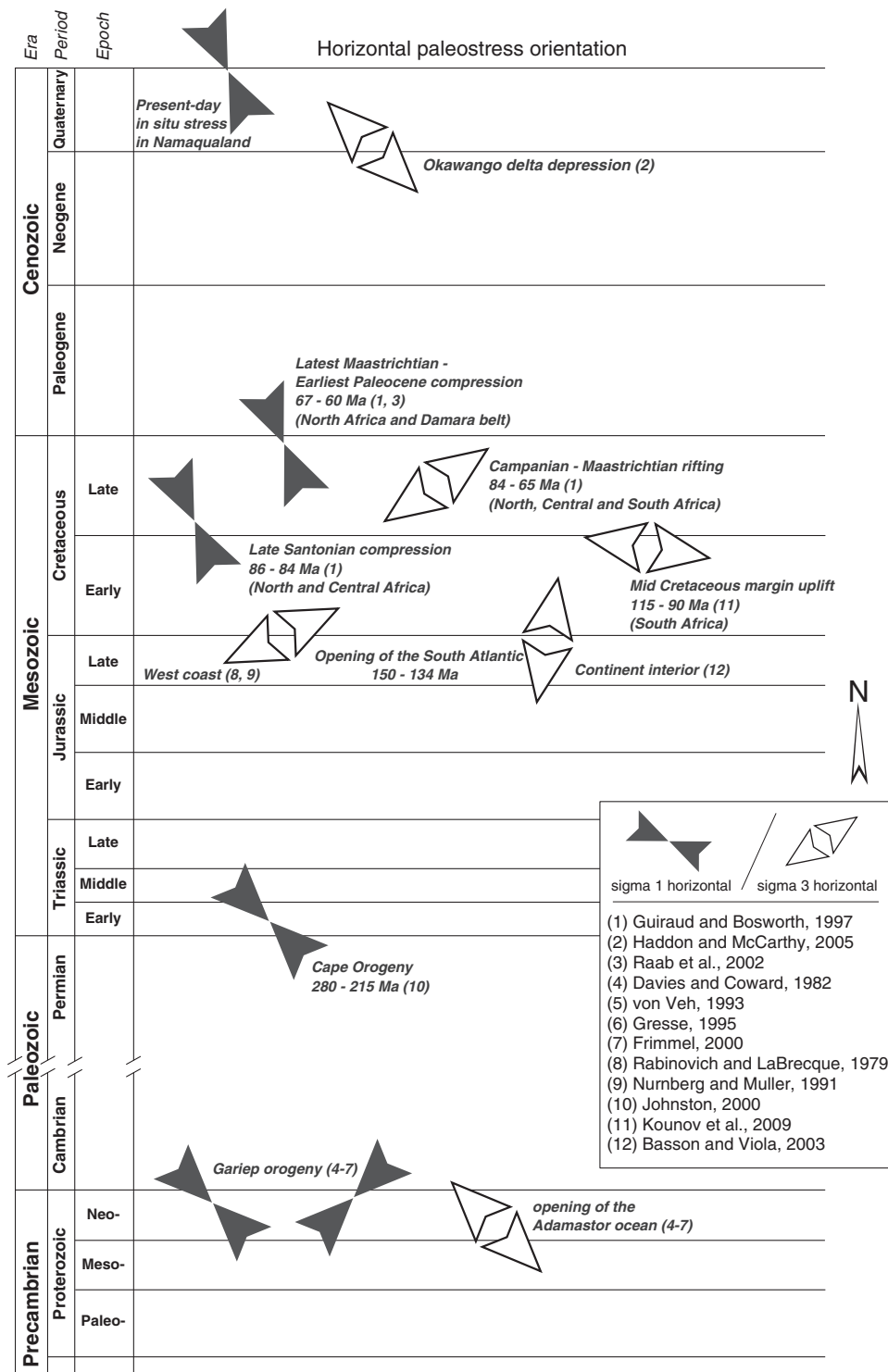


Fig. 18. Compilation of the known tectonic events that have affected Africa. Sources used to generate the compilation are listed in the figure.

3 km of crust across the western coastal zone in front of the escarpment in South Africa (e.g. Brown et al., 2002; Kounov et al., 2008, 2009; Tinker et al., 2008). Fission track analysis has helped constrain a distinct period of accelerated cooling in the coastal domain during this time interval, which is reasonably associated with enhanced exhumation and erosion. Onshore denudation was coupled with substantial uplift offshore Namaqualand, where seismic profiles and boreholes show significant erosional horizons marking the Aptian regression (121–112 Ma; e.g. Brown et al., 1995; Gerrard and Smith, 1983). Several lines of evidence indicate the tectonic character of

this episode and its regional significance (see Kounov et al., 2009 for a review). We propose that this denudation episode caused the exhumation of the NMP in the study area. The formation of the fluvial Dasdap Formation described by Brandt et al. (2003) is probably associated with this episode.

5.3. Late Cretaceous evolution

As the area was exhumed to the surface, it underwent significant weathering leading to the development of thick saprolites (silicified

and kaolinized, weathered metamorphic rocks topped by sediments) and paleosols. The crater fill sediments developed on top the Late Cretaceous (77–54 Ma) volcanic pipes of the Gamoep suite contain ferricrete and silcrete-kaolinite palaeosol clasts suggesting that weathering was active in the area already prior to this volcanic activity. On the other hand, the fact that these sediments are also weathered indicates that intense surface processes continued the pervasive weathering of the NMP well into the Cenozoic. We can therefore suggest that the rocks presently exposed at the surface in the study area were at or near the surface already in the Mid Cretaceous, consistent with the preservation of pollens, dinosaur bones and frogs (de Wit et al., 1992; Tyson and Partridge, 2000) as fossils in the Late Cretaceous crater infill deposits.

Following these lines of reasoning, the remaining part of the reconstruction of the brittle evolution is interpreted as being related to the post-Mid Cretaceous geological evolution. Unfortunately, the addition of time constraints to our newly derived paleostress tensors for that time interval is made particularly challenging by the fact that there is no clear sequence of tectonic events known so far from the west coast of South Africa. Several tectonic phases have been instead reported from within the African continent for the Late Cretaceous (e.g. Delvaux et al., 2011; Guiraud, 1998; Guiraud and Bosworth, 1997; Raab et al., 2002). During the Late Santonian (85–83 Ma), a generally NW-SE oriented, remarkable compression phase has been recognized in large parts of the African continent and it has been linked genetically to a major change in the position of the poles of rotation for the opening of the Atlantic Ocean. This event was also synchronous with the onset of the separation between India and Madagascar (Plummer, 1996; Schlich, 1982). Based on the remarkably similar orientation of the greatest stress axis and on the available time constraints, we suggest that compressional *Tensor 7* (Fig. 13; D7, Fig. 16) represents the far-field expression of such event in South Africa and in central-southern Namibia.

The next major tectonic event widely documented almost in the whole African plate is an NE-SW extensional episode of Campanian-Maastrichtian age (ca. 80–70 Ma). According to Guiraud and Bosworth (1997) it can be recognized by the rejuvenation and opening of numerous rift basins along the continental margin as well as in the plate interior. Along the eastern margin of southern Africa, local rifting events related to the overall evolution of the Indian Ocean have also been reported in addition to localized subsidence along the southern margin of the continent (Dingle et al., 1983). A number of normal faults from our study area, some of which are probably older reactivated structures, constrain indeed a phase of NE-SW extension (*Tensor 9*, Fig. 14) and are therefore assigned to this tectonic episode of continent-scale importance (D8, Fig. 16). The evidence that this tectonic phase postdates the Late Santonian compression (D7) is found in the field relationships presented, for example, in Fig. 8a, where SE dipping low-angle reverse faults are cut by a set of NW-SE trending normal faults.

The Campanian-Maastrichtian time interval is also the age of the peak of alkaline volcanic activity in the Gamoep cluster of Namaqualand (77–66 Ma; Phillips et al., 2000). Huge traps of flow basalts of the same age are recognized offshore between Africa and Madagascar (e.g. Raillard, 1990).

A further compressional event accommodating NNW-SSE to N-S shortening within the African continent has been described for the end of the Cretaceous and the beginning of the Paleogene (e.g. Janssen et al., 1995; Maurin and Guiraud, 1993; Raab et al., 2002). Most of the deformation assigned to this phase is reported from the northern part of the continent in the hinterland of the Alpine orogen (e.g. Guiraud and Bosworth, 1997). In southern Africa, though, Maastrichtian compression is also described, for example along the Damara belt in central Namibia by the reactivation of major Pan-African shear zones (e.g. the Waterberg thrust, Raab et al., 2002). We tentatively suggest

that *Tensor 8* (Fig. 13) is the local expression of this tectonic stage (D9, Fig. 17). In fact, shortening directions that are ascribed to this event across the continent are rather heterogeneously oriented, in contrast to, for example, the Late Santonian shortening phase (see Guiraud and Bosworth, 1997). It should be noticed, however, that it is possible that the fault slip data used to compute this tensor derive from faulting related to more than just one single tectonic phase. The sorting and separation of these possible multiple phases were probably unsuccessful due to the small misorientation angle between their principal stress axes. Close inspection of the fault data stereoplots shows in fact the existence of structures with almost N-S oriented striations (Fig. 13).

Irrespective of whether this subset is really internally homogeneous, the post-Late Cretaceous age of all its individual components is confirmed by the fact that the tensor was derived from reverse faults mapped within the Gamoep suite volcanic breccia pipe and faults from the “Total weathered” dataset.

5.4. Cenozoic and present-day stress state

Several studies have dealt with the Cenozoic geomorphic evolution of southern Africa and, indirectly, have addressed issues related to tectonisms during this time interval (e.g. Andreoli et al., 1996; Burke, 1996; Burke and Gunnell, 2008; Moore, 1999; Partidge, 1998; Partridge and Maud, 1987). No study, however, has proposed direct structural constraints on the proposed sequence of events and only morphologic or sedimentological features were used to infer and constrain large-scale tectonic processes affecting southern Africa. Conclusions remain thus general and disputable, do not rely on clear and robust structural evidence and often describe only very local events. The evolution of southern Africa during the last ~30 Ma is generally related to the nucleation and amplification of several epeirogenic flexure axes and the connected reorganization of the river drainage systems (e.g. Moore, 1999; Partridge and Maud, 1987). Some have attributed this evolution to dynamic processes in the mantle and the formation of the African Superswell (e.g. Burke, 1996; de Wit, 2007; Doucoure and de Wit, 2003).

Some attempts have been made toward a unifying review of the neotectonic evolution in South Africa, either by building on available, although limited, stress and structural/geomorphologic and geophysical data (Andreoli et al., 2009; Bird et al., 2006; Viola et al., 2005) or on the spatial distribution of seismic epicenters and sparse geodetic data (Hartnady, 2002). On a first account, it would seem that the two approaches lead to different conclusions. Whereas, for example, Bird et al. (2006) modeled the present stress pattern in southern Africa as arising from the resistance of the unbroken lithosphere to the relative rotation of the incipient Somalia plate away from Africa plate, the alternate model views the African plate in southern Africa as having already been fragmented in a number of small plates separated by a network of diffuse boundaries (cf. DeMets et al., 2010). In describing the evidence for late Cenozoic (neotectonic) faulting in the Vaalputs area, including the ~4 km wide, 25 km long Santab fault swarm, Brandt et al. (2005) explored instead the possibility that such features originated from the eastward migration of a coast-parallel axis of uplift akin, not unlike the model proposed by Gilchrist et al. (1994).

In consideration of the scarcity of confirmed data, only one tensor was assigned to the Cenozoic tectonic evolution of the area. The last tensor (*Tensor 10*, Fig. 14) obtained from the “weathered” fault set is tentatively attributed to the Pliocene-Early Pleistocene NW-SE oriented extensional tectonic phase reported in the Kalahari basin (D10 in Fig. 17; e.g. Haddon and McCarthy, 2005; McCarthy et al., 2002). This stage is related to the propagation of the East African Rift System into southern Africa and formation of local fault-bounded depressions (Modisi et al., 2000).

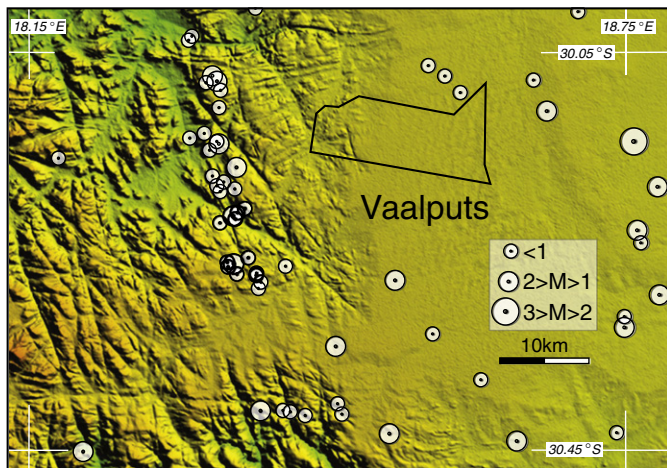


Fig. 19. Distribution of seismic epicenters located in Namaqualand and in the Bushmanland Plateau from 1989 to 31 December 2010, as recorded by two trial TELS Stations sited within the Vaalputs radioactive waste disposal facility (Necsa catalog; Scheepers and Andreoli, 2004; Scheepers, 2011, personal communication).

6. Continued fault reactivation and faulting style

Our reconstruction suggests up to ten distinct deformation episodes, all of which are constrained by the inversion of statistically robust outcrop fault slip datasets (Fig. 17). So many events were in part accommodated by important structural reactivation during the >500 Myr long brittle evolution of this region. Evidence of reactivation is documented by, for example, the rose diagram of Fig. 6, which indicates very limited dispersion of the orientations of the steep brittle faults inherited from the Pan African history, which controlled the overall subsequent development of the large-scale brittle grain of Namaqualand. The paleostress state evolution summarized in Fig. 17 also demonstrates important reactivation through the presence of similarly oriented faults in different deformation episodes bearing striations with significantly different trends caused by renewed faulting along the preexisting planes.

This in turn confirms the idea that, once formed, a fault-fracture represents a zone of intrinsic mechanical weakness, which is repeatedly exploited during subsequent deformation phases to accommodate further increments of strain. The fracture saturation state of the NMP and the progressively decreasing ratio between fragmentation and jostling with time (*sensu* Munier and Talbot, 1993; Viola et al., 2009) inhibited therefore the nucleation and development of new brittle structures with orientations other than the overall NNW-SSE grain (inherited from the early Pan African evolution) that characterizes the NMP.

Viola et al. (2005) presented evidence of significant fault reactivation also from the offshore domain in the Orange basin, where the alignment of mud volcanoes and the interpretation of seismic lines shot at high angle to the alignment trend were used to suggest the presence of strike-slip faulting along NNW-SSE steep faults. In addition, they also proposed that strike-slip faults root down into- and reactivated older listric normal faults genetically linked to the local opening of the Atlantic Ocean. Viola et al. (2005) interpreted NNW-SSE-oriented wrench faulting as a neotectonic phenomenon, expression of the so-called “Wegener anomaly” (Fig. 17; Andreoli et al., 1996; Bird et al., 2006).

The results of our fault slip tendency analysis, calculated from the present-day stress as constrained by the *in situ* stress determinations of Nieuwoudt and Rozendaal (1990) (Fig. 17), are in agreement with these observations and allow to better define the concept of fault reactivation and to link it to the present-day seismicity of the area (Andreoli et al., 2009). At all depths considered, slip tendency values are highest for conjugate faults striking WNW-ESE and NNW-SSE and

dipping between 50° and 90° . The highest computed slip tendency values are above or close to 1, suggesting that faults with such orientations are prone to failure in the present stress field. This orientation prediction strengthens the suggestions of Viola et al. (2005) with regard to neotectonic strike-slip faulting along steep to sub-vertical NNW-SSE and conjugate direction trends. Moreover, it is also in agreement with the location of a cluster of seismic events recorded and located immediately to the west of Vaalputs (Fig. 19; Andreoli et al., 2009; J. Scheepers, pers. comm.), where numerous earthquakes up to magnitude 4 are aligned along a ca. 25 km long NNW-SSE seismogenic weak fault zone with a remarkable morphologic signature.

Finally, we notice how the faulting style in the weathered profiles is remarkably different from that observed and documented within the fresh NMP basement. Fault-slip data derived from the latter are invariably associated with steep to sub vertical strike-slip faults, often arranged in conjugate sets with very tight acute angles. On the other hand, faults and fractures from the weathered horizons are predominantly low-angle thrusts and normal faults. The sub-horizontal fossil weathered horizons may have acted as a weak mechanical boundary such that post-weathering deformation was preferentially localized along faults and fractures subparallel to weathering front in the kaolinite-enriched weathered mesas (e.g. Angerer et al., 2011).

7. Conclusions

This study has gathered and compiled for the first time a significant data set of brittle structures in Namaqualand, western South Africa. Remote sensing, field work and stress tensor inversion have been used to propose a robust conceptual model that accounts for more than 500 Myr of brittle deformational history along the western margin of South Africa. This long-lasting, complex brittle evolution stems from the generation of steep strike-slip fractures and faults in the NMP during the Neoproterozoic Pan African orogeny, when the Gariep Mobile Belt docked against the rigid Namaqualand foreland as part of the process that formed super continent Gondwana. The subsequent and continued reactivation of these pre-existing, inherited structures (up to the present time, as documented by the local present-day seismic activity) has controlled vehemently the accommodation of younger increments of strain, both compressional and extensional, that resulted predominantly from the Mesozoic evolution of the plate and the opening of the Atlantic Ocean. The paleostress tensors summarized in Fig. 17 describe these multiple episodes of fragmentation and reactivation, and, furthermore, tie in reasonably well with the known geological evolution of the region. Comparison of our results with other episodes of deformation known to have affected the African plate (Fig. 18) allows the better characterization of a number of important tectonic events at the continental scale and yields useful insights into the mechanisms that controlled the opening of the South Atlantic Ocean.

Acknowledgments

Research described in this report was funded by NGU and Statoil through ‘The African Plate’ project. The authors are also grateful to Necsa, the South African National Research Foundation (grant FUN NRF 70728) and the Inkaba ye Africa research initiative (sub-project: Post Gondwana tectonics from Namaqualand to the Kalahari) for providing financial and traveling assistance. This paper is the publication nr. 65 of the Inkaba ye Africa project. Ingrid Stengel and Andrew Logue are thanked for their great support in the field, stimulating discussions and friendship. As always, special thanks go to the staff of Necsa and of the Vaalputs Radioactive Waste Disposal Facility for their hospitality and logistical support. The reviewers Donald Wise and Francesco Mazzarini provided constructive and inspiring comments. Fabrizio Storti handled very efficiently the review process.

References

- Anderson, E.M., 1951. The Dynamics of Faulting and Dyke Formation with Applications to Britain. Oliver & Boyd, Edinburgh, p. 191.
- Andreoli, M.A.G., Doucoure, M., Van Bever Donker, J., Brandt, D., Andersen, N.J.B., 1996. Neotectonics of southern Africa: a review. *Africa Geosciences Review* 3 (1), 1–16.
- Andreoli, M.A.G., Hart, R.J., Ashwal, L.D., Coetzee, H., 2006. Correlation between U, Th content and metamorphic grade in the Western Namaqualand belt, South Africa, with implications for radioactive heating of the crust. *Journal of Petrology* 47, 1095–1118.
- Andreoli, M.A.G., Viola, G., Kounov, A., Scheepers, J., Heidbach, O., Stengel, I., 2009. History of stress at Vaalputs, Namaqualand, South Africa: evidence for a Mid-Cretaceous “Wegener-type Orogeny” in western southern Africa. 6 pp. 11th SAGA Biennial Technical Meeting and Exhibition, Mbabane, Swaziland.
- Angelier, J., 1979. Determination of the mean principal direction of stresses for a given fault population. *Tectonophysics* 56, 17–26.
- Angelier, J., Tarantola, A., Valette, B., Manoussis, S., 1982. Inversion of field data in fault tectonics to obtain the regional stress; I. single phase fault populations: a new method of computing the stress tensor. *Geophysical Journal of the Royal Astronomical Society* 69, 607–621.
- Angerer, T., Greiling, R.O., Avigad, D., 2011. Fabric development in a weathering profile at a basement-cover interface, the sub-Cambrian peneplain, Israel: implications for decollement tectonics. *Journal of Structural Geology* 33, 819–832.
- Basson, I.J., Viola, G., 2003. Structural overview of selected Group II kimberlite dyke arrays in South Africa: implications for kimberlite emplacement mechanisms. *South African Journal of Geology* 106, 375–394.
- Basson, I.J., Viola, G., 2004. Passive kimberlite intrusion into actively dilating dyke-fracture arrays: evidence from fibrous calcite veins and extensional fracture cleavage. *Lithos* 76, 283–297.
- Bird, P., Ben Avraham, Z., Schubert, G., Andreoli, M., Viola, G., 2006. Patterns of stress and strain rate in southern Africa. *Journal of Geophysical Research* 111, B08402. doi:10.1029/2005JB003882.
- Bott, M.H.P., 1959. The mechanics of oblique slip faulting. *Geological Magazine* 96, 109–117.
- Brandt, D., Andreoli, M.A.G., McCarthy, T.S., 2003. Mesozoic fluvial deposits on a rifted continental margin near Vaalputs, Namaqualand, South Africa. *South African Journal of Geology* 106, 1–16.
- Brandt, D., Andreoli, M., McCarthy, T.S., 2005. The Late Mesozoic paleosols and Cenozoic fluvial deposits at Vaalputs, Namaqualand, South Africa. Possible depositional mechanism and their bearing on the evolution of the continental margin. *South African Journal of Geology* 108, 267–280.
- Brown, R.W., 1992. A fission track thermochronology study of the tectonic and geomorphic development of the sub-aerial continental margins of southern Africa. PhD thesis, La Trobe University, Melbourne, Australia.
- Brown, L.F., Benson, J.M., Brink, G.J., et al., 1995. Sequence stratigraphy in offshore South African Divergent Basins. An Atlas on Exploration for Cretaceous Low-stand Traps by SOEKOR (Pty) Ltd. AAPG Studies in Geology, 41. 184 pp.
- Brown, R.W., Gallagher, K., Gleadow, A.J.W., Summerfield, M.A., 2000. Morphotectonic evolution of the South Atlantic margins of Africa and South America. In: Summerfield, M.A. (Ed.), *Geomorphology and Global Tectonics*. John Wiley and Sons Ltd., pp. 255–284.
- Brown, R.W., Summerfield, M.A., Gleadow, A.J.W., 2002. Denudation history along a transect across the Drakensberg Escarpment of southern Africa derived from apatite fission track thermochronology. *Journal of Geophysical Research* 107 (B12), 2350. doi:10.1029/2001JB000745.
- Brynard, H.J., 1988. A petrological and geochemical study regarding the suitability of the Vaalputs Radioactive Waste Disposal Facility. Ph.D. thesis, University of Pretoria, Pretoria, South Africa.
- Brynard, H.L., Levin, M., Botha, J., 1996. Importance of natural attenuation of contaminants as parameter in site selection. *African Geoscience Review* 3, 17–30.
- Burke, K., 1996. The African Plate. *South African Journal of Geology* 99, 341–409.
- Burke, K., Gunnell, Y., 2008. The African Erosion Surface: a continental-scale synthesis of geomorphology, tectonics, and environmental change over the past 180 million years. *Geological Society of America, Memoir* 201, 66.
- Byerlee, J.D., 1978. Friction of rocks. *Pure and Applied Geophysics* 116, 615–629.
- Cornelissen, A.K., Verwoerd, W.J., 1975. The Bushmanland kimberlites and related rocks. In: Ahrens, L.H., Dawson, J.B., Duncan, A.R., Erlank, A.J. (Eds.), *Physics and Chemistry of the Earth, Vol. 9*. Pergamon Press, Oxford, pp. 71–80.
- Cornell, D.H., Thomas, R.J., Moen, H.F.G., Reid, D.L., Moore, J.M., Gibson, R.L., 2006. The Namaqua-Natal Province. In: Johnson, M.R., Anhaeusser, C.R., Tomas, R.J. (Eds.), *The Geology of South Africa*. Geological Society of South Africa, Johannesburg/Council for Geoscience, Pretoria, pp. 325–379.
- Davies, C.J., Coward, M.P., 1982. The structural evolution of the Gariep Arc in southern Namibia. *Precambrian Research* 17, 173–198.
- de Wit, M.J., 2007. The Kalahari Epeirogeny and climate change: differentiating cause and effect from core to space. *South African Journal of Geology* 110, 367–392.
- de Wit, M.J., Ransome, I.G.D., 1992. Regional inversion tectonics along the southern margin of Gondwana. In: de Wit, M.J., Ransome, I.G.D. (Eds.), *Inversion Tectonics of the Cape Fold Belt, Karoo and Cretaceous Basins of Southern Africa*. Balkema, Rotterdam, pp. 15–21.
- de Wit, M.C.J., Ward, J.D., Spaggiari, R., 1992. A reappraisal of the Kangnas dinosaur site, Bushmanland, South Africa. *South African Journal of Science* 88, 504–507.
- Delvaux, D., Sperner, B., 2003. New aspects of tectonic stress inversion with reference to the TENSOR program. In: Nieuwland, D.A. (Ed.), *New Insights into Structural Interpretation and Modelling*: Geological Society of London Special Publication, 212, pp. 75–100.
- Delvaux, D., Kadima, E., Litke, R., Sachse, V., Glasmacher, U., Bauer, F., Sebagenzi, S., 2011. Late Cretaceous subsidence and tectonic inversion in the Congo Basin from paleostress, organic matter maturation and thermochronometric studies of archived core and outcrop samples. EUG 2011. Vienna.
- DeMets, C., Gordon, R.G., Argus, D.F., 2010. Geologically current plate motions. *Geophysical Journal International* 181, 1–80.
- Dingle, R.V., Siesser, W.G., Newton, A.R., 1983. *Mesozoic and Tertiary Geology of Southern Africa*. Balkema, Rotterdam. 375 pp.
- Doucoure, C.A., de Wit, M.J., 2003. Old inherited origin for the present near bimodal topography of Africa. *Journal of African Earth Sciences* 36, 371–388.
- Drake, H., Tullborg, E.-L., Page, L., 2009. Distinguish multiple events of fracture mineralization related to far-field orogenic effects in Paleoproterozoic crystalline rocks, Simpevarp area, SE Sweden. *Lithos* 110, 37–49.
- Eagles, G., 2007. New angles on South Atlantic opening. *Geophysical Journal International* 166, 353–361.
- Eales, H.V., March, J.S., Cox, K.G., 1984. The Karoo igneous province: an introduction. In: Erlank, A.J. (Ed.), *Petrogenesis of the Volcanic Rocks of the Karoo Province*: Geological Society of South Africa Special Publication, 13, pp. 1–26.
- Eglington, B.M., 2006. Evolution of the Namaqua-Natal Belt, southern Africa – a geochronological and isotope geochemical review. *Journal of African Earth Sciences* 46, 93–111.
- Etchecopar, A., Vassuer, G., Daignieries, M., 1981. An inverse problem in microtectonics for the determination of stress tensors from fault striations analysis. *Journal of Structural Geology* 3, 51–65.
- Frimmel, H.E., 2000. The Pan-African Gariep Belt in Southwestern Namibia and Western South Africa. *Communications of the Geological Survey of Namibia* 12, 197–209.
- Frimmel, H.E., Frank, W., 1998. Neoproterozoic tectono-thermal evolution of the Gariep Belt and its basement, Namibia and South Africa. *Precambrian Research* 90, 1–28.
- Gerrard, I., Smith, G.C., 1983. Post-Paleozoic succession and structure of the southwestern African continental margin. In: Watkins, J.S., Drake, C.L. (Eds.), *Studies in Continental Margin Geology*: AAPG, Memoir, 34, pp. 49–74.
- Gilchrist, A.R., Henk, K., Beaumont, C., 1994. Post-Gondwana geomorphic evolution of southwestern Africa: implications for the controls on landscape development from observations and numerical experiments. *Journal of Geophysical Research* 99, 12211–12228.
- Gresse, P.G., 1994. Strain partitioning in the southern Gariep Arc as reflected by sheath folds and stretching directions. *South African Journal of Geology* 97, 52–61.
- Gresse, P.G., 1995. Transpression and transection in the late Pan-African Vanrhynsdorp foreland thrust-fold belt, South Africa. *Journal of African Earth Sciences* 21, 91–105.
- Gresse, P.G., Fitch, F.J., Miller, J.A., 1988. ⁴⁰Ar/³⁹Ar dating of the Cambro-Ordovician Vanrhynsdorp tectonite in southern Namaqualand. *South African Journal of Geology* 91, 257–263.
- Guiraud, R., 1998. Mesozoic rifting and basin inversion along the northern African-Arabian Tethyan margin: an overview. *Hydrocarbon Geology of North Africa*: Geol. Soc. London, Spec. Publ., Vol. 132, pp. 217–229.
- Guiraud, R., Bosworth, W., 1997. Phanerozoic geodynamic evolution of northeastern Africa and the northwestern Arabian platform. *Tectonophysics* 315, 73–108.
- Haddon, I.G., McCarthy, T.S., 2005. The Mesozoic–Cenozoic interior sag basins of Central Africa: the Late-Cretaceous–Cenozoic Kalahari and Okavango basins. *Journal of African Earth Sciences* 43, 316–333.
- Hancock, P.L., 1985. Brittle microtectonics: principles and practice. *Journal of Structural Geology* 7, 437–457.
- Hartnady, C.J.H., 2002. Earthquake hazard in Africa: perspectives on the Nubia-Somalia boundary. *South African Journal of Science* 98, 425–428.
- Haughton, S.H., 1931. On a collection of fossil frogs from the clay at Banke. *Transactions of the Royal Society South Africa* 19, 233–249.
- Hawkesworth, C., Kelley, S., Turner, S., le Roex, A., Storey, B., 1999. Mantle processes during Gondwana break-up and dispersal. *Journal of African Earth Sciences* 28, 239–261.
- Janssen, M.E., Stephenson, R.A., Cloethingh, S., 1995. Temporal and spatial correlations between changes in plate motions and the evolution of rifted basins in Africa. *Geological Society of America Bulletin* 107 (11), 1317–1332.
- Johnson, M.R., Anhaeusser, C.R., Thomas, R.J., 2006. *The geology of South Africa*. Geological Society of South Africa, Johannesburg, Council of Geoscience, Pretoria. 691 pp.
- Johnston, S.T., 2000. The Cape Fold Belt and Syntaxis and the rotated Falkland Islands: dextral transpressional tectonics along the southwest margin of Gondwana. *Journal of African Earth Sciences* 31, 51–63.
- Jourdan, F., Féraud, G., Bertrand, H., Watkeys, M.K., 2007. From flood basalts to the inception of oceanization: example from the ⁴⁰Ar/³⁹Ar high resolution picture of the Karoo large igneous province. *Geochemistry, Geophysics, Geosystem* 8, Q02002. doi:10.1029/2006GC001392.
- King, L.C., King, L.A., 1959. A reappraisal of the Natal monocline. *South African Geographical Journal* 41, 15–30.
- Kooi, H., Beaumont, C., 1994. Escarpment evolution on high-elevation rifted margins: insights derived from a surface-processes model that combines diffusion, advection and reaction. *Journal of Geophysical Research* 99, 12,191–12,209.
- Kounov, A., Viola, G., de Wit, M.J., Andreoli, M., 2008. A Mid Cretaceous paleo-Karoo River valley across the Knersvlakte plain (northwestern coast of South Africa): evidence from apatite fission-track analysis. *South African Journal of Geology* 111, 409–420.
- Kounov, A., Viola, G., de Wit, M.J., Andreoli, M., 2009. Tectonic evolution and denudation of the Atlantic passive margin: new insights from apatite fission-track analysis on the Western coast of South Africa. In: Lisker, F., Ventura, B., Glasmacher, U. (Eds.), *Thermochronological Methods: from Paleotemperature Constraints to Landscape Evolution Models*. Geological Society, London. Special Publications.

- Levin, M., 1988. A geohydrological appraisal of the Vaalputs radioactive waste disposal facility in Namaqualand, South Africa. Ph.D. thesis, University of the Free State, Bloemfontein, South Africa.
- Lithgow-Bertelloni, C., Silver, P., 1998. Dynamic topography, plate driving forces and the African superswell. *Nature* 395, 269–272.
- Mabbutt, J.A., 1955. Pediment land forms in little Namaqualand. *South African Geographical Journal* 121, 77–83.
- Maurin, J.-C., Guiraud, R., 1993. Basement control in the development of the Early Cretaceous West and Central African Rift System. *Tectonophysics* 228, 81–95.
- McCarthy, T.S., Moon, B.P., Levin, M., 1985. Geomorphology of the western Bushmanland plateau, Namaqualand, South Africa. *South African Geographical Journal* 67, 160–178.
- McCarthy, T.S., Smith, N.D., Ellery, W.N., Gumbricht, T., 2002. The Okavango Delta-semiarid alluvial-fan sedimentation related to incipient rifting. In: Renaut, S., Ashley, G.M. (Eds.), *Sedimentation in Continental Rifts. Society of Economic Palaeontologists and Mineralogists (SEPM): Special Publication, No. 73*, pp. 170–193.
- Modisi, M.P., Atekwana, E.A., Kampunzu, A.B., 2000. Rift kinematics during the incipient stages of continental extension: evidence from nascent Okavango rift basin, northwest Botswana. *Geology* 28, 939–942.
- Moore, A.E., 1999. A reappraisal of epeirogenic flexure axes in southern Africa. *South African Journal of Geology* 102, 363–376.
- Moore, A.E., Verwoerd, W.J., 1985. The olivine melilitite-kimberlite-carbonatite suite of Namaqualand and Bushmanland, South Africa. *South African Journal of Geology* 88, 281–294.
- Morris, A.P., Ferrill, D.A., Henderson, D.B., 1996. Slip tendency analysis and fault reactivation. *Geology* 24, 275–278.
- Munier, R., Talbot, C.J., 1993. Segmentation, fragmentation and jostling of cratonic basement in and near Åspö, southeast Sweden. *Tectonics* 12, 713–727.
- Nieuwoudt, A.P.C., Rozendaal, A., 1990. In situ stress determinations in mines located in two major structural domains in South Africa. *Static and Dynamic Considerations in Rock Engineering*. Balkema, Rotterdam, pp. 213–222.
- Nürnberg, D., Müller, R.D., 1991. The tectonic evolution of the South Atlantic from late Jurassic to present. *Tectonophysics* 191, 27–53.
- Nyblade, A., Robinson, S., 1994. The African superswell. *Geophysical Research Letters* 21, 765–768.
- Partridge, T.C., 1998. Of diamonds, dinosaurs and diastrophism: 150 million years of landscape evolution in southern Africa. *South African Journal of Geology* 101, 167–184.
- Partridge, T.C., Maud, R.R., 1987. Geomorphic evolution of southern Africa since the Mesozoic. *South African Journal of Geology* 90, 179–208.
- Partridge, T.C., Maud, R.R., 1989. The end-Cretaceous event: new evidence from the southern hemisphere. *South African Journal of Science* 85, 428–430.
- Partridge, T.C., Maud, R.R., 2000. *The Cenozoic of Southern Africa*. Oxford University Press, New York, pp. 3–18.
- Pether, J., Roberts, D.L., Ward, J.D., 2000. Deposits of the West Coast. In: Partridge, T.C., Maud, R.R. (Eds.), *The Cenozoic of Southern Africa*, pp. 33–54.
- Petit, J.P., 1987. Criteria for the sense of movement on fault surfaces in brittle rocks. *Journal of Structural Geology* 9, 597–608.
- Phillips, D., Kiviets, G.B., Biddulph, M.G., Madav, M.K., 2000. Cenozoic volcanism. In: Partridge, T.C., Maud, R.R. (Eds.), *The Cenozoic of Southern Africa*. Oxford University Press, pp. 182–197.
- Plummer, Ph.S., 1996. The Amirante ridge/trough complex: response to rotational transform rift/drift between Seychelles and Madagascar. *Terra Nova* 8, 34–47.
- Raab, M.J., Brown, R.W., Gallagher, K., Carter, A., Weber, K., 2002. Late Cretaceous reactivation of major crustal shear zones in northern Namibia: constraints from apatite fission track analysis. *Tectonophysics* 349, 75–92.
- Rabinovich, P.D., LaBrecque, J., 1979. The Mesozoic South Atlantic Ocean and evolution of its continental margin. *Journal of Geophysical Research* 84, 5973–6002.
- Raillard, S., 1990. Le marges de l'Afrique de l'Est et les zones de fracture associées: Chaîne de Davie et Ride du Mozambique. Campagne MD-60fMACAMO-II. Ph.D. Thesis, Univ. Pierre et Marie Curie, Paris, 272 pp.
- Reid, D.L., Rex, D.C., 1994. Cretaceous dikes associated with the opening of the South Atlantic: the Mehlberg dike, northern Richtersveld. *South African Journal of Geology* 97, 135–145.
- Reid, D.L., Ransome, I.G.D., Onstott, T.C., Adams, C.J., 1991. Time of emplacement and metamorphism of Late Precambrian mafic dykes associated with the Pan-African Gariep orogeny, Southern Africa: implications for the age of the Nama Group. *Journal of African Earth Science* 13, 531–541.
- Saintot, A., Stephens, M., Viola, G., Nordgulen, Ø., 2011. Fault slip data and paleostress field reconstruction of brittle deformation in the south-western Fennoscandian Shield, Forsmark, Sweden. *Tectonics* 30, TC4002. doi:10.1029/2010TC002781.
- Scheepers, J., Andreoli, M.A.G., 2004. The Seismological record of Vaalputs up to 31st December 2003. *Necsa Open File Report, GEA-1650*, Pretoria. 99 pp.
- Schlich, R., 1982. The Indian Ocean: aseismic ridges, spreading centres and basins. In: Nairn, A.E., Stehli, E.G. (Eds.), *The Ocean Basins and Margins: The Indian Ocean*, Vol. 6. Plenum.
- Scholtz, A., 1985. The palynology of the upper lacustrine sediments of the Arnot pipe, Banke, Namaqualand. *Annales of the South African Museum* 95, 1–109.
- Smith, M.J., WISE, S.M., 2007. Problems of bias in mapping linear landforms from satellite imagery. *International Journal of Applied Earth Observation and Geoinformation* 9, 65–78. doi:10.1016/j.jag.2006.07.002.
- Smith, C.B., Allsopp, H.L., Kramers, J.D., Hutchinson, G., Roderick, J.C., 1985. Emplacement ages of Jurassic-Cretaceous South African kimberlites by the Rb–Sr method on phlogopite and whole rock samples. *Transactions of the Geological Society of South Africa* 88, 249–266.
- Tinker, J., de Wit, M., Brown, R., 2008. Mesozoic exhumation of the southern Cape, South Africa, quantified using apatite fission track thermochronology. *Tectonophysics*. doi:10.1016/j.tecto.2007.10.009.
- Trumbull, R.B., Reid, D.L., de Beer, C., van Acken, D., Romer, R.L., 2007. Magmatism and continental breakup at the west margin of southern Africa: a geochemical comparison of dolerite dikes from northwestern Namibia and the Western Cape. *South African Journal of Geology* 110, 477–502.
- Tyson, P.D., Partridge, T.C., 2000. The evolution of Cenozoic climates. In: Partridge, T.C., Maud, R.R. (Eds.), *The Cenozoic of Southern Africa*, Oxford University Press: New York; 406 pp.
- Unrug, R., 1997. Rodinia to Gondwana: the geodynamic map of Gondwana Supercontinent assembly. *GSA Today* 7, 1–6.
- Viola, G., Andreoli, M., Ben-Avraham, Z., Stengel, I., Reshef, M., 2005. Offshore mud volcanoes and onland faulting in southwestern Africa: neotectonic implications and constraints on the regional stress field. *Earth and Planetary Science Letters* 231, 147–160.
- Viola, G., Venvik Ganerød, G., Wahlgren, C.-H., 2009. Unravelling 1.5 Gyr of brittle deformation history in the Laxemar-Simpevarp area, SE Sweden: a contribution to the Swedish site investigation study for the disposal of highly radioactive nuclear waste. *Tectonics* 28, TC5007. doi:10.1029/2009TC002461.
- Viola, G., Mattila, J., Zwingmann, H., Todd, A., Raven, M., 2011. Structural and K/Ar illite geochronological constraints on the brittle deformational history of the Olkiluoto region, SW Finland. Working Report 2011–37. Posiva OY, Finland.
- Von Veh, M.W., 1988. The stratigraphy and structural evolution of the Late Proterozoic Gariep belt in the Sendelingsdrif - Annisfontein area, northwestern Cape Province. M.Sc. thesis 174p. University Cape Town, South Africa.
- Von Veh, M.W., 1993. The stratigraphy and structural evolution of the Late Proterozoic Gariep Belt in the Sendelingsdrif-Annisfontein area, Northwestern Cape Province. *Precambrian Research Unit, University of Cape Town Bulletin*, p. 38. 174 p.
- Wallace, R.E., 1951. Geometry of shearing stress and relation to faulting. *Journal of Geology* 59, 118–130.
- Waters, D.J., 1989. Metamorphic evidence for the heating and cooling path of Namaqualand granulites. In: Daly, J.S., Cliff, R.A., Yardley, B.W.D. (Eds.), *Evolution of Metamorphic Belts*: London: The Geological Society Special Publication, 43, pp. 357–363.